4

Radiation Protection and Dosimetry in PET and PET/CT

Jocelyn E.C. Towson and Stefan Eberl

Positron emission tomography (PET) imaging is one of the more challenging and interesting areas of radiation safety in diagnostic medicine as a result of its combination with computed tomography (CT). Hybrid systems employ current generation multislice CT (MSCT) (also called multidetector CT, MDCT) scanners, rather than CT units purpose-designed for PET/CT systems. A diagnostic CT scan, including the use of contrast as required, can therefore be acquired with the PET scan in the one imaging session. Alternatively, a low-dose "nondiagnostic" CT may be acquired just to provide data for attenuation correction and an anatomical frame of reference for interpretation of the PET image. In future, scanners for specialized applications such as radiation treatment planning and cardiac, breast, and brain imaging may affect the exposure of employees through changes in their close contact with patients. In any event, an understanding of the radiation safety issues, to keep clinical and occupational exposures as low as reasonably achievable (ALARA) and to design facilities, is required for the modalities in combination.

CT dose to the patient can vary widely depending on the system and protocol. It is therefore important to use a protocol that is appropriate for the purpose of the PET/CT scan (1, 2). If the CT is used for diagnostic purposes as well as attenuation correction and coregistration of PET data, its contribution to dose should be the same as if the system were a stand-alone CT. If not, there is considerable scope to reduce CT dose without compromising the accuracy of the quantitative PET data or the localization of abnormal isotope distribution. Even though the majority of PET/CT studies are for oncology referrals, it is desirable to minimize radiation dose to healthy tissue particularly when considering disease in remission, serial follow-up studies, and referrals for nonmalignant disease. Reduced radiopharmaceutical activities and low-dose nondiagnostic CT protocols are particularly appropriate for children and pregnant women.

The International Commission on Radiological Protection (ICRP) has evolved a system for the safe use of radiation, including definitions of various dosimetric quantities and recommended dose limits for radiation protection. However, some of the terminology is esoteric, and neither the quantities nor dose limits have universal acceptance. The ICRP is currently moving to clarify its terminology while maintaining the recommended dose limits of 1990 shown in Table 4.1 (3, 4). In this chapter, gray (Gy) is used for *absorbed dose* to organs and tissues from medical exposures and sievert (Sv) is used for *equivalent dose* to organs and tissues from occupational and public exposures. The two quantities are numerically identical for beta, gamma, and X-rays. *Effective dose*, a convenient index of risk to the whole person from nonuniform exposure whether clinical or occupational or public, is also expressed in sieverts. Radiation dose from diagnostic medical procedures ranges from less than 1 to a few tens of mGy or mSv. (Corresponding dose in rads or rems can be obtained by dividing a value in mGy or mSv by 10, or multiplying a value in Gy or Sv by 100.) Exposures from artificial sources or human practices can be viewed in the context of 'background' radiation. The effective dose from naturally occurring sources has a broad distribution, depending on the local geology and habitat. The world average is 2.4 mSv $year^{-1}$ with a mode of 2 mSv $year^{-1}$ and a 90th percentile of 3 mSv $year^{-1}$ (5).

The risk of radiation at the dose levels associated with occupational, public, and diagnostic medical exposures is essentially the stochastic risk of cancer. The risk from exposure at low doses and dose rates can be expressed as an excess lifetime risk of mortality of 5% Sv^{-1} to a population of all ages and both sexes and 4% Sv^{-1} to adults of working age, although the ICRP in its Draft 2005 Recommendations is considering the use of incidence rather than mortality, which would roughly double these risk coefficients (3, 4). In the Life Span Study (LSS) of the atomic bomb survivors in Japan, the risk per unit dose in the range 0 to 200 mSv (of interest for radiation protection and frequent CT procedures) is consistent with the linear response seen over the full range, 0 to 2 Sv. For both mortality and incidence, the best estimate of threshold

Table 4.1. Dose limits recommended by the International Commission on Radiological Protection (ICRP).

	Occupational	Public
Effective dose	20 mSv year^{-1}, averaged over 5 years and not more than 50 mSv in any 1 year	1 mSv year^{-1}
Equivalent dose		
Lens of the eye	150 mSv year^{-1}	15 mSv year^{-1}
Skin	500 mSv year^{-1}	50 mSv year^{-1}
Hands and feet	500 mSv year^{-1}	—

Source: Data from ICRP Publication 60 (3).
From Valk PE, Bailey DL, Townsend DW, Maisey MN. Positron Emission Tomography: Basic Science and Clinical Practice. Springer-Verlag London Ltd 2003, p. 266.

dose is 0 with an upper-bound 90% confidence limit between 60 and 100 mSv (6). An effective dose of 200 mSv to adults from their occupation adds about 1% in theory to the normal risk of dying from cancer of about 25%.

The data from the LSS are complemented by epidemiologic data from medical exposures, ranging from the trivial to high-dose radiotherapy, which also highlight the increased susceptibility of children (7). The age-dependence of risk is illustrated in Figure 4.1 (3, 8). There is understandable concern about the exposure to infants and children from CT (9–11). Concern about exposures in children, particularly for superficial radiosensitive organs including the lens of the eye, thyroid, and breast/anterior chest wall, can be extrapolated to exposures in utero, where the risk of developmental abnormalities is added to a presumed risk of cancer similar to that of the postnatal infant (3, 8, 12–14), as summarized in Table 4.2. A review of all published studies on childhood cancer following fetal irradiation concluded that a fetal dose of 10 to 20 mGy can increase the risk by about 40%, the risk being greatest in the third trimester (15). As the baseline mortality rate for childhood cancer is so low, the effect of a fetal dose of 10 mGy is marginal, reducing the probability of *not* developing childhood cancer from 99.7% to 99.6% (12). A fetal dose of 25 mGy, quite possible with PET/CT, may double the natural risk (about 1 in 1,300 in the United Kingdom) of fatal childhood cancer, although it would have very little effect on lifetime risk (about 1 in 4) thereafter (8).

Radiation from PET and CT Sources

PET Radionuclide Emissions

In terms of energy deposition in tissue, PET radionuclides have more in common with the radionuclides used for therapy than those used for diagnostic imaging. The amount of energy deposited locally or at a distance from disintegrating atoms in an infinite medium is indicated by the equilibrium absorbed dose constant, delta (Δ), as shown in Table 4.3 for a selection of radionuclides used for diagnosis and therapy (16, 17). Positrons, being nonpenetrating charged particles, deposit their energy locally and account for most of the dose to the organs and tissues

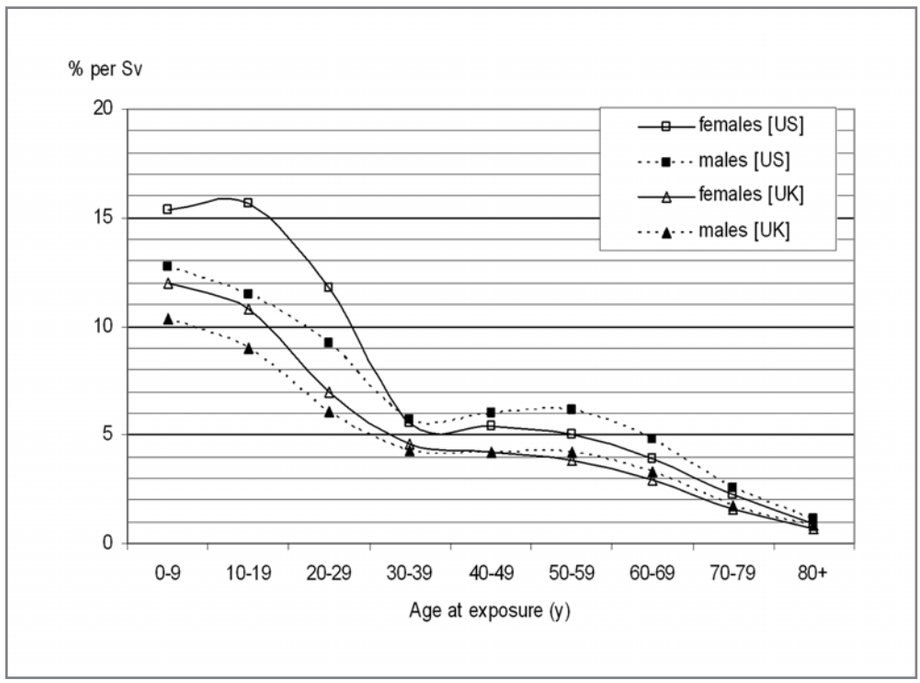

Figure 4.1. Age-dependent excess lifetime risk of fatal cancer following radiation exposure. [Data from ICRP 60 (International Commission on Radiological Protection) (U.S. data) and NRPB (National Radiological Protection Board) (U.K. data) (3, 8).]

Table 4.2. Risk of radiation exposure in utero and the normal risks of pregnancy.

Effect	Gestational age at exposure (weeks postconception)	Threshold (Gy)	Risk (Gy^{-1})	Normal prevalence or incidence
Lethality	1–3 inclusive		Minimal	
Spontaneous abortion				>15% to term
Congenital abnormalities, growth retardation	4–7 inclusive	>0.1	50%	6%
Severe mental retardation	8–15 inclusive	>0.1	40%	0.5%
	16–25 inclusive	>0.2	10%	
Reduced IQ:	8–15 inclusive	>0.1	30 points	
Mental retardation				3%
Cancer	4 until term			
Incidence to 15 years		—	6%	0.077%
Mortality to 15 years		—	3%	0.154%
Mortality lifetime			~12%	~25%
Genetic disorders	4 until term		2.4%	8%

Source: Data from NRPB (8), ICRP (12).

of PET patients. Photons emitted in the annihilation of the positrons are penetrating and account for the exposure of persons nearby. The *activity* of a radioactive substance is measured by the number of radioactive atoms that disintegrate in a second, the becquerel (Bq) being an activity of one disintegration per second. The activity of ^{18}F-fluorodeoxyglucose (FDG) administered to adult patients is generally in the range from 200 to 750 MBq, or roughly 5 to 20 millicuries (mCi). (Activity in mCi is determined by dividing the value in MBq by 37.) The influence of half-life on the energy available from the total decay of a radioactive source is evident in Table 4.3. The short half-lives of clinical PET radionuclides limit the internal radiation dose to patients and the external radiation dose to persons who come in contact with the patient some time after the PET scan. However, they confer no particular benefit on PET staff, who must contend each day with high dose rates from patients and many patients to be scanned.

External exposure to gamma radiation is the most significant pathway for occupational exposure in PET facilities. The high dose rates from PET radionuclides relative to other radionuclides used for diagnostic imaging result from their high photon energy (511 keV) and photon yield (typically 197%–200%). Other potential pathways are these:

- A skin dose from surface contamination
- A deep dose from bremsstrahlung generated in lead or other material of high atomic number
- A superficial dose from positrons emitted from the surface of uncovered sources
- An immersion dose from a release of radioactive gas into the room air

The dose rate at a distance in air from a source of radiation can be expressed in various terms depending on the application. Dose rate constants at a distance of 1 m from a 1 GBq "point" source of various radionuclides are given

Table 4.3. Energy from decay of selected nuclear medicine radionuclides.

	Equilibrium absorbed dose constant, Δ[a] (g Gy MBq^{-1} h^{-1})				
	Nonpenetrating Δn–p	Penetrating Δp	Total Δ	$T_{1/2}$	Energy from total decay of 1 MBq (μJ)
^{11}C	0.227	0.588	0.815	20.3 mins	397
^{13}N	0.281	0.589	0.870	10.0 mins	209
^{15}O	0.415	0.589	1.004	2.07 mins	50
^{18}F	0.139	0.570	0.709	1.83 h	1,868
^{90}Y	0.539	–	0.539	2.7 days	50,295
^{99m}Tc	0.010	0.072	0.082	6.0 h	708
^{131}I	0.109	0.219	0.328	8.05 days	91,250

[a]Data from Society of Nuclear Medicine MIRD Committee (16, 17).
Source: From Valk PE, Bailey DL, Townsend DW, Maisey MN. Positron Emission Tomography: Basic Science and Clinical Practice. Springer-Verlag London Ltd 2003, p. 267.

Table 4.4. Dose rate constants for radionuclides used for diagnostic imaging.

	Air kerma rate constant[a] ($\mu Gy\ m^2\ GBq^{-1}\ h^{-1)}$	Ambient dose equivalent H*(10) rate constant[a] ($\mu Sv\ m^2\ GBq^{-1}\ h^{-1}$)	Deep tissue dose rate (photons) at 1 m[b] (1 GBq point source) ($\mu Sv\ h^{-1}$)	Superficial tissue dose rate (electrons) at 1 m[b] (1 GBq point source) ($\mu Sv\ h^{-1}$)
^{11}C	140	170	170	11,700
^{13}N	140	170	170	10,800
^{15}O	140	170	170	10,800
^{18}F	140	170	160	10,800
^{67}Ga	19	27	25	0
^{99m}Tc	14	21	23	0
^{111}In	75	88	89	8
^{123}I	36	44	47	0
^{131}I	53	66	66	7,700
^{201}Tl	10	17	18	0

Note: "Ambient dose equivalent" is the operational quantity corresponding to "deep tissue dose" at a depth of 10 mm. "Superficial tissue dose" refers to a depth of 0.07 mm, the average depth of the basal cell layer in skin.
[a]Photons >20keV. Data from Groenewald and Wasserman (18).
[b]Photons. Data from Delacroix et al. (19).
[c]Electrons. Data from Delacroix et al. (19).
Source: From Valk PE, Bailey DL, Townsend DW, Maisey MN. Positron Emission Tomography: Basic Science and Clinical Practice. Springer-Verlag London Ltd 2003, p. 267.

in Table 4.4 (18, 19). The rate constants for photons can be used to check the response of survey meters, whether calibrated for dose in air (Gy) or dose in tissue (Sv), to a reference source of known activity. The superficial tissue dose rates in Table 4.4 are for betas and electrons only and may substantially overestimate actual dose rates because they do not allow for absorption in the source and walls of the container. However, they do indicate that skin and eye doses from open PET sources could be reduced significantly by interposing a barrier as thick as the maximum beta range (see properties in Table 4.5) (19, 20). Internal exposure from radionuclide intakes, which can be estimated by counting activity in biologic samples or the body, are not generally a concern in PET. Continuous air sampling should be used to monitor occupied areas where there may be a risk of inhaling PET gases.

CT Radiation Measurement and Dose Quantities

The primary fan beam of X-rays produced by a CT system is intense and tightly collimated (21). The energy spectrum is relatively "hard" in radiology terms, with a beam quality of about 5 to 6 mm aluminum half-value layer and an effective energy of about 70 keV for a 120-kVp beam, although soft in comparison with the 511-keV annihilation photons of PET. Secondary radiation comprises leakage from the X-ray tube housing and scattered radiation from photon interactions with the patient, the detec-

Table 4.5. PET radionuclide properties for radiation protection.

	β+ yield per disintegration	β+ E_{max} (MeV)	Range in glass[a] (mm)	Range in plastic[a] (mm)	Skin dose rate: 1 kBq in 0.05 mL[a] ($mSv\ h^{-1}$)
^{11}C	1.0	0.960	1.6	3.0	1.1
^{13}N	1.0	1.199	2.1	4.0	1.2
^{15}O	1.0	1.732	3.4	6.4	1.4
^{18}F	0.97	0.634	0.9	1.7	0.8
Attenuation of annihilation photons (broad beam)		Z_{on} Z_{eff}	Density ($g\ cm^3$)	Mean HVL[b] (cm)	Mean TVL[b] (cm)
	Concrete	—	2.2	6.4	22
	Concrete	—	3.2	3.1	11
	Iron	26	7.87	1.6	5.5
	Tungsten	74	19.30	0.32	1.1
	Lead	82	11.35	0.56	2.0

[a]Positrons. Data from Delacroix et al. (19).
[b]Photons 500 keV. Data from Wachsmann and Drexler (20).

tors, or any other object in the primary beam. Leakage radiation is at the maximum end of the energy spectrum, and the intensity is limited by regulatory control to a low level. Scatter photons are emitted in all directions and make a substantial contribution to dose in and beyond the primary beam. The radiation dose from a single rotation of the CT tube is therefore not confined to the slice width but extends on either side with a characteristic peaked distribution in the z-direction of the scanner axis. The dose from a single rotation is represented by the *CT dose index* (CTDI), which assigns the whole of the deposited energy to the slice. CTDI is measured in air on the axis of rotation, or at the center and periphery of a standard phantom positioned in the center of the gantry. There are two standard acrylic phantoms, both at least 14 cm in length: 32 cm in diameter for the body, 16 cm in diameter for the head and pediatrics. The *weighted* $CTDI_w$ represents the average dose throughout a slice in the phantom and is characteristic of the machine, whereas the *volume* $CTDI_{vol}$ allows for noncontiguous slices and is therefore a better representation of dose during a scan. The total energy deposited in the patient, and hence the stochastic risk, from a complete scan sequence is represented by the *dose length product* (DLP). $CTDI_w$, $CTDI_{vol}$, and DLP are applicable to axial or spiral scan modes and single- or multislice systems (22).

In contrast to film radiography, there is no inherent warning of overexposure from a CT image. Improvements in tube rating that allow longer scans at higher current without exceeding the heat capacity are fully exploited in MSCT systems. Tissue dose may be up to tens of mGy, associated with very low levels of image noise. The radiation dose delivered to the patient is determined by the system type/model, the examination protocol, and the patient's shape and size. It is impossible to quote a valid "one-size-fits-all" dose for CT procedures.

The key responsibility of the operator is to decide the appropriate level of image quality for the diagnostic purpose and then to select a suitable protocol with minimal dose to the patient. The operator has some choice, but the relationship between image quality—contrast, noise, voxel resolution, and artifacts—and dose is complex. For spiral CT the operator selects tube current mA, rotation time, table feed per rotation (although these may be interlinked by the manufacturer to automatically maintain total mAs for the scan length), kVp, beam width, and scanned length. These values are required input for CT dose calculation programs. Dose can also be influenced indirectly by the choice of matrix size, filter, and windowing, which might cause the operator to increase exposure in an effort to improve image quality.

Preinstalled CT protocols for different applications were intended, in the past, to give the best image quality and improved diagnostic confidence in a competitive market with less emphasis on radiation protection. Manufacturers of MSCT systems have responded to concerns about patient dose by implementing automatic exposure control (AEC), ECG-gated tube current for cardiac CT, age- and weight-related protocols, on-screen display of weighted or volume CTDI, DLP, and specification of geometric efficiency for each imaged slice width option (both z-axis efficiency, being the proportion of the beam width in the z-direction seen by the detectors, and detector efficiency, being the proportion of the array area that is occupied by active detectors excluding septa). AEC is currently achieved in various ways by automatic modulation of tube current (ATCM) according to body size

Summary of CT Dose Definitions

CTDI is the integral of the absorbed dose profile measured in air on the axis of rotation, or at the center and periphery of a standard phantom positioned in the center of the gantry, divided by the nominal slice width (or MSCT beam width) for a single rotation in axial mode. CTDI subscripts indicate the medium in which the dose index is measured and/or quoted, the method of measurement and calculation:

- $CTDI_{air}$ is measured in air on the axis of rotation and quoted as dose to air.
- $CTDI_{100}$ is measured in an acrylic phantom with a 100-mm-long ion chamber and quoted as dose to air. [$CTDI_{FDA}$, as originally defined by the U.S. Food and Drug Administration (FDA), is measured in 14 contiguous sections of a tissue-equivalent phantom and quoted as dose to tissue-equivalent material. Factors are available to convert to $CTDI_{100}$ (23)].
- The weighted $CTDI_w$ represents the average dose throughout a slice from a single rotation in axial mode, calculated from $CTDI_{100}$ measured at the center and the mean $CTDI_{100}$ measured at 10-mm depth at four equally spaced positions around the periphery of a standard phantom:

$$CTDI_w = 1/3\ CTDI_{100,c} + 2/3\ CTDI_{100,p}\ (\text{in mGy})$$

- The volume $CTDI_{vol}$ allows for noncontiguous slices. The overlap or gap between slices is given by the pitch, that is, the couch increment/total slice width in axial mode, or travel feed per rotation/total beam width in spiral mode:

$$CTDI_{vol} = CTDI_w/\text{pitch}\ (\text{in mGy})$$

- ${}_nCTDI$ (all versions) are normalized to mGy per mAs (or sometimes 100mAs).
- The DLP is related to the $CTDI_w$ and scanned length L:

$$DLP = CTDI_w \times L/\text{pitch} = CTDI_{vol} \times L\ (\text{in mGy cm})$$

or

$$DLP = {}_nCTDI_w \times L \times \text{effective mAs}\ (\text{in mGy cm})$$

where effective mAs = mAs per rotation/pitch.

If there is more than one scan sequence in the examination, the DLP values are summed.

overall and along the z-axis, based on the preliminary scout view radiograph. ATCM also uses angular modulation, either sinusoidal or based on attenuation at projections from the previous rotation. ATCM increases dose in the region of metal implants but only to an extent similar to the dose reduction from using ATCM instead of fixed mA (24). Each manufacturer has a slightly different approach to ATCM, so it is important that the operator understands the connection between image quality, scan parameters, and dose when selecting the ATCM option (25). ATCM is a valuable means of reducing dose while maintaining image quality, presuming the operator selects an appropriate noise level or mA for a standard patient. Operators may err on the side of high image quality rather than low dose, as suggested by simulation studies in which noise was added to clinical CT images without impairing diagnostic quality (26). The challenge for PET/CT is to select a reference current or noise level for ATCM that is optimal for the purpose of the CT. If a diagnostic CT image is not required, tube current and time could be reduced by as much as 50% in some circumstances.

Independent evaluation reports on similar scanners, for example, 16-slice units (27), are available to assist anyone contemplating the purchase of a PET/CT scanner. As summarized by Nagel (28), the system characteristics that affect dose are the power waveform to the X-ray generator, the selectable tube current range and steps, the inherent beam filtration from the tube assembly, additional beam-shaping filters, the distance from the tube focus to the axis of rotation, the total slice or beam width (collimated at the tube, not selected at the detector array), the detector type and array, the scanner configuration, the scan field of view, and the selectable scan angle during a full rotation.

Medical Exposures

Estimation of Organ and Tissue Dose from PET

Despite the high energy of decay, the radiation dose from PET tracers, although limited by the short physical half-life, is similar to that from many imaging procedures using single photon emissions. The dose may also be limited by the maximum amount of activity that can be administered to the patient without taxing the response of the detector system, which is a particularly important consideration when the scanner is operated without septa in three-dimensional (3D) mode. For a whole-body study with a scanner with bismuth germanate (BGO) detectors operating in 3D mode, the administered activity should be less than 250 to 400 MBq, depending on the scanner and uptake period. Even with fast cerium-doped lutetium oxyorthosilicate (LSO) or gadolinium oxyorthosilicate (GSO) detectors, careful consideration needs to be given to the injected activity. Patient-based noise-equivalent count rate (NECR) estimates can provide insight into maximum injected activities that should be used with the scanner to avoid operating beyond the peak NECR point (29, 30). Furthermore, near peak NECR the incremental improvement in signal to noise (S/N) with increasing activity is very small. Based on NECR analysis for an LSO scanner, the injected activity required to achieve peak S/N (or peak NECR) is more than 70% larger than that required to operate at 95% peak S/N (31). In other words, a very large increase (>70%) in injected activity yields only a small increase of 5% in S/N when operating close to the peak NECR of the scanner. Thus, there is potential for a considerable reduction in injected activity without noticeable degradation of image quality. Weight-based injected activities have also been suggested with very high activities (>600 MBq) for heavy patients (32, 33), but patient-based NECR analysis and image quality assessment of 3D whole-body studies have shown that little improvement in image quality can be gained from increasing the injected activity in heavy patients (29–31), and it is preferable to increase scan acquisition time. The larger injected activities could, however, result in increased radiation exposure to the patients and staff.

Radiopharmaceutical dose estimates are calculated using the methodology developed by the Medical Internal Radiation Dose (MIRD) Committee of the Society of Nuclear Medicine (34). Software for this purpose is available from the Radiation Dose Assessment Resource (RADAR) professional group at www.doseinfo-radar.com/OLINDA.html (35). The MIRD method requires an estimate of the spatial and temporal distribution of radioactivity in the body, which can be obtained from organ activity-time curves from images at various time points. Biokinetic models are used to model the movement of activity through anatomic and physiologic compartments. The cumulative activity in a "source" organ is multiplied by a dose factor to give the dose to a "target" organ. The total dose to each target organ is obtained by summing the contributions from all the identified source organs. Dose factors for PET radionuclides, and more than 800 others, can be accessed on the RADAR website www.doseinfo-radar.com, an extensive electronic resource which also includes a description of the various physiologic models and anthropomorphic phantoms for Monte Carlo modeling used in their derivation (36).

Image fusion allows a more accurate determination of organ uptake of PET radiopharmaceuticals than conventional gamma camera methods can do for non-PET radiopharmaceuticals. Tomography overcomes the need for geometric mean imaging with planar detectors and subtraction of "background" counts for under- and overlying tissues. PET/CT coregistration and edge contouring allow anatomically correct and consistent selection of regions of interest. Finer PET resolution reduces partial volume errors, and high sensitivity and attenuation correction of PET data gives better accuracy for radioactive tissue concentration. For example, organ delineation in combined

PET and MRI images has been used to measure the distribution of a carbon-11 ligand in maternal and fetal organs of macaque monkeys weighing less than 9 kg (37) and of FDG in adults (38).

Effective dose is calculated from the individual organ and tissue doses using the tissue weighting factors recommended by the ICRP in 1990 (3) (that replaced those used to calculate "effective dose equivalent" and which it may review again to reflect the latest estimates of organ/tissue susceptibility to radiation damage). Dose coefficients for radiopharmaceuticals have been published by the ICRP and others and are also available on the RADAR site (36, 39–43). Dose coefficients for various PET radiopharmaceuticals in the U.S. and British Pharmacopoeia and the ICRP compendia are shown in Table 4.6 (39, 41–46).

The ICRP noted the difficulties of applying conventional dosimetry methods to very short lived PET tracers and foreshadowed the development of novel ad hoc methods of dose estimation (39). For example, the radioactivity may not last long enough to allow true equilibration of the tracer in body compartments, or the highest dose may be received by organs or tissues such as the trachea or walls of major blood vessels that have not been assigned a specific tissue weighting factor. The dose estimates for injected ^{15}O-water and inhaled ^{15}O-gases are cases in point (47–49). The MIRD Committee has developed its own biokinetic model for the bladder and kidneys (50). Optional bladder parameters (static, dynamic) are relevant to FDG dosimetry because bladder dose can be reduced by hydration and frequent voiding (51). For the very short lived nuclides, biokinetics have little influence

Table 4.6. Dose coefficients for various positron emission tomography (PET) tracers listed in Pharmacopeia and ICRP.

	USP 2000	BP 2004	Effective dose (mSv GBq^{-1})	Organ of maximum dose	Maximum organ dose (mGy GBq^{-1})	Uterus dose (mGy GBq^{-1})	Source of data
^{11}C							
Acetate	✓	✓	5.0	Heart	100	2.0	RIDIC
			3.5	Liver	14	1.4	ICRP53/A4
Amino acids, generic			5.5	Pancreas	41	3.5	ICRP53/A5
Brain receptors, generic			4.5	Bladder	32	4.5	ICRP53/A6
Methionine	✓	✓	7.4	Bladder	91	5.7	ICRP53/A4
Methyl thymidine			3.5	Liver	32	1.5	ICRP80
Raclopride	✓	✓	5.3 (EDE)	—	—	—	Wrobel
Spiperone			5.3	Liver	22	2.2	ICRP53, ICRP80
Thymidine			2.7	Kidneys	11	2.4	ICRP80
All substances, realistic maximum			11	Bladder	170	9.2	ICRP53/A7
^{13}N							
Ammonia	✓	✓	2.0	Bladder	8.1	1.9	ICRP53, ICRP80
^{15}O							
CO gas		✓					ICRP53, ICRP80
20-min breath hold			0.81	Lungs	3.4	0.3	
1-h continuous			0.55	Lungs	2.3	0.2	
Water	✓	✓	1.1	Heart	1.9	0.35	ICRP53/A5 [a]
O_2 gas		✓					ICRP53, ICRP80
20-min breath hold			0.37	Lungs	2.4	0.057	
1-h continuous			0.4	Lungs	2.6	0.068	
^{18}F							
Fluoride	✓		24	Bone, RBM	40	19	ICRP53, ICRP80
FDG	✓	✓	19	Bladder	170	20	ICRP80
FDG			n/a	Bladder	73	n/a	MIRD19 [b]
FDG			29	Bladder	310	(19)	Deloar
Fluorodopa	✓		25	Bladder	300	28	ICRP53/A4 [c]
Amino acids, generic			23	Pancreas	140	17	ICRP53/A5

[a] ^{15} O-water: ICRP53 Addendum 5 is correction to ICRP80.
[b] ^{18} F-FDG MIRD19 is based on different biokinetics (45) to ICRP80.
[c] ^{18} F-Fluorodopa brain uptake is doubled by carbidopa pretreatment (46).
RBM, red bone marrow.
Source: Data from ICRP Publication 53 and Addenda; RIDIC; MIRD (44); Wrobel et al. (52); Deloar et al. (38).

beyond the initial distribution and uptake phases. Two time points for measuring organ activity were deemed to be sufficient for a study of ^{11}C compounds in an animal model (52).

Estimation of Organ and Tissue Dose from CT

In contrast to the whole-body dose distribution from most radiopharmaceuticals, CT dose is essentially confined to the scanned region of interest, although the difference is minimal for whole-body PET/CT examinations. A significant component of CT dose comes from photon scatter interactions with tissues in the primary beam (there is little point in shielding adjacent regions of the body with lead aprons during a CT scan). It can be quite high immediately adjacent to the scanned section and falls off quickly with distance beyond the scan limits. Total scatter dose depends on the irradiated volume: the body cross section, beam width, pitch, and scanned length. Figure 4.2 illustrates the increasing dose to the uterus as the PET/CT scanner bed moves in a craniocaudal direction through the CT gantry. Other sources of external exposure to a patient are comparatively small:

- Leakage radiation, although "harder" than the primary beam spectrum after penetrating the tube shielding, is limited by regulation to a dose rate of less than 1 mGy h^{-1} at 1 m under maximum output operating conditions. During a MSCT scan lasting a minute or so, tissue dose from leakage radiation would be less than a few tens of μGy.
- The effective dose from the preliminary scout view (a rapid, narrow beam anterposterior AP and/or lateral planar image) used to set z-axis limits, and modulate tube current in some systems, is of the order of tens to a few hundreds of μSv.
- PET systems without CT and some with CT use a radionuclide source for attenuation correction of PET image data, either coincidence (germanium-68/gallium-68) or single photon (cesium-137). The short duration of the exposure and the source collimation result in an insignificant dose to the patient (53).

CT dose estimates sufficient for most purposes can be calculated with software employing data sets of organ dose in an anthropomorphic phantom, such as CT-Expo.xls available from www.mh-hannover.de/kliniken/radiolgie/str_04.html and CTDosimetry.xls from www.impactscan.org (54, 55). The CTDosimetry.xls calculator from the ImPACT center uses Monte Carlo datasets from the National Radiological Protection Board (56), which were calculated from measurements made in 1989 on scanners that are no longer in use. To overcome this limitation, the calculator is periodically updated by matching the characteristics of newly released scanners to the most suitable NRPB-250 Head and Body datasets by a process that combines the $CTDI_c$ and $CTDI_p$, normalized to $CTDI_{air}$ (www.impactscan.org/dosesurveysummary.htm). The Monte Carlo approach can be extended from phantom models to voxelized patient data (57). Unlike a radiopharmaceutical dose, a transmission scan dose can be validated using small thermoluminescent dosimeters (TLD) in an anthropomorphic phantom. For example, the

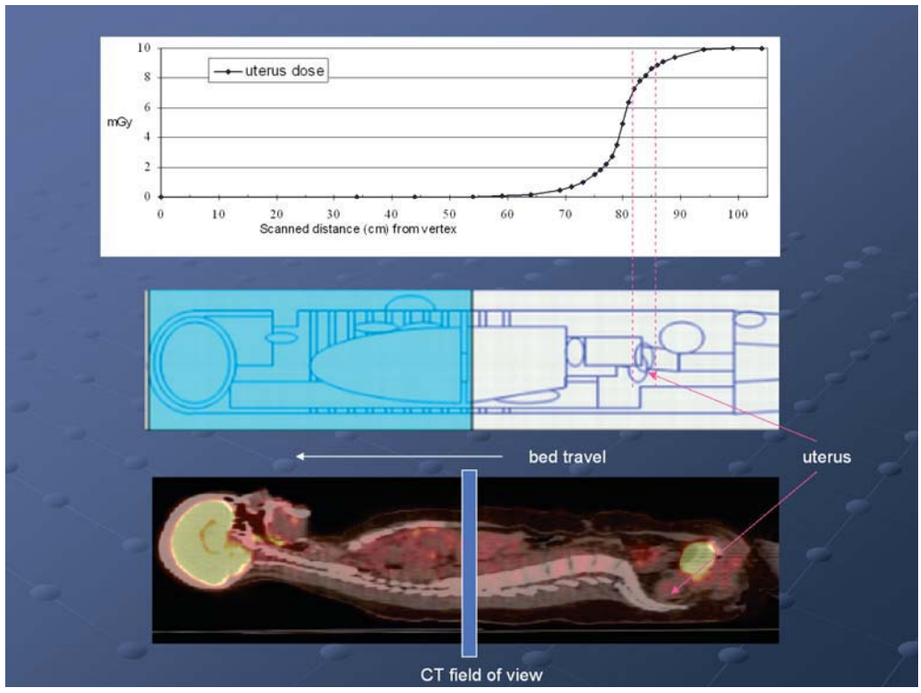

Figure 4.2. Progressive dose to uterus from primary and scattered computed tomography (CT) radiation during whole-body scan. Calculated for Siemens Sensation 16, 120 kVp, 100 mAs, 24-mm total beam width, pitch 1, no allowance for automatic tube current modulation (55).

effective dose values of 8.81 mSv and 18.97 mSv for two CT procedures from TLD measurements in a Rando Alderson phantom (58) are in good agreement with the values of 8.6 mSv and 17 mSv obtained for the same CT system and factors with dose calculation software (55).

With CT dose calculation programs, the user selects the upper and lower limits on the diagram of an anthropometric phantom corresponding to the scanned length and enters the scanner manufacturer/model, the scanned region (head or body), and the exposure factors. The output lists organ and tissue doses and the effective dose. When comparing protocols, dose to critical organs is useful, for example, thyroid, breast, uterus, gonads, and lens of the eye (the PET/CT gantry cannot be angled to avoid the eyes). The relative CTDI for the selected beam collimation (useful for comparing multislice options), $CTDI_w$, $CTDI_{vol}$, and DLP may also be given. Dose calculators give a conservative estimate if the effect of ATCM is not taken into account. A closer estimate may be obtained if the mA value averaged for the total scan length is entered instead of the nominal or maximum mAs.

Most PET/CT scanners sold at this time (2005) incorporate a MSCT system. When multislice systems were introduced, it was reported that the average effective dose increased by 30% for a scan of the head and 150% for scans of the chest and abdomen, to 1.2, 10.5, and 7.7 mSv respectively, compared with a conventional single-section scanner (59). The increase was ascribed to longer scanned length and more scan phases achievable with the increased speed and tube rating of these systems. Other surveys have noted a fall in dose as operators lowered mAs and increased pitch to maximize coverage (60, 61). In general, MSCT dose should be similar to single-slice scanners using the same technique factors, except for an increase in dose at the very thin slice options due to overbeaming on the detector array (62, 63). Useful commentaries on PET/CT and MSCT dose issues can be found on the ImPACT website www.impactscan.org (64, 65).

In summary:

CT protocols should be optimized for the purpose of the scan, diagnostic or nondiagnostic.

Dose from nondiagnostic CT can be reduced by reducing the mAs (or "effective mAs" adjusted for pitch) to approximately half the usual settings for a diagnostic CT, using a slightly lower kVp for children than adults, and avoiding thin beam widths or overlapping slices.

Whole-body protocols specific to patient weight, pregnant women, and children should be used.

Dose should be calculated locally for the particular system and all protocols, paying careful attention to what happens for various settings. For example, what happens on a particular system with selection of slice widths, ATCM, or pitch? Is the screen display of $CTDI_w$ really $CTDI_{vol}$?

Radiation Dose to Patients from PET and PET/CT Examinations

Radiation dose in diagnostic CT has attracted considerable attention in recent years, in particular for pediatric examinations. It can be very misleading to quote a "representative" dose for a CT scan because of the wide diversity of applications, protocols, and CT systems; this also applies to the CT component of a PET/CT study. For example, a whole-body scan may or may not include the head, a conventional diagnostic quality CT may or not be required, and the CT may or may not be repeated with radiologic contrast (66). The effective dose could range from approximately 5 to 80 mSv for these options. It is therefore advisable to estimate CT dose specific to the scanner and protocol.

Furthermore, surveys have demonstrated that dose for any given type of CT examination can vary by an order of magnitude or more at different clinics (22, 61, 67–69). The ICRP has recommended the use of "diagnostic reference levels" for radiology and nuclear medicine for guidance in limiting radiation dose while achieving a suitable image quality, which is important for CT because dose levels are relatively high (70). Reference levels apply to an easily measured quantity and to a representative group of patients, not to an individual. Levels may be set by professional bodies or national or international organizations, for example, at the 75th percentile of values reported in surveys. For nuclear medicine, the reference quantity is the activity of the radiopharmaceutical administered to an adult patient. For CT, the historical reference quantities are $CTDI_w$ in the head or body phantom and DLP for a particular application. In recent recommendations, $CTDI_{vol}$ replaces $CTDI_w$ (71), and reference levels are given separately for single/dual-slice systems and for MSCT, and for adults and children (61). Selected CT reference levels are shown in Table 4.7 (23, 61, 71, 72). No reference levels for PET/CT imaging have been recommended, which is hardly surprising given the ongoing evolution of hybrid systems and the various ways in which the images are used.

The Adult Patient

Organ dose and effective dose in adult patients from a PET scan can be estimated from the dose coefficients in Table 4.6. Effective dose is generally in the range of 5 to 10 mSv, which is comparable to the dose from many nuclear medicine procedures. If CT dose calculation software is not available, a simpler estimation of effective dose from CT of a specific region can be obtained by multiplying the DLP recorded on the scanner console (or calculated from the $CTDI_w$) by a conversion factor: head 0.0023, neck 0.0054, chest 0.017, abdomen 0.015, and pelvis 0.019 mSv mGy^{-1} cm^{-1} (23). Effective dose estimates for PET, PET/CT, nuclear medicine, and CT examinations for similar purposes are shown in Table 4.8 (41, 73–75).

Table 4.7. Selected diagnostic reference levels for single slice and multislice computed tomography (SSCT and MSCT) dose for adults protocols.

	Protocol	Reference	Level
NRPB (2005)	Head (cerebrum)	DLP	SSCT 760 / MSCT 930 mGy cm
		$CTDI_{vol}$	SSCT 55 / MSCT 65 mGy
	Lymphoma survey	DLP	SSCT 760 / MSCT 940 mGy cm
	Lung	$CTDI_{vol}$	SSCT 10 / MSCT 12 mGy
	Abdomen/pelvis	$CTDI_{vol}$	SSCT 12 / MSCT 14 mGy
MSCT (2004]	Head	$CTDI_{vol}$	MSCT 60 mGy
	Chest	$CTDI_{vol}$	MSCT 10 mGy
	Abdomen	$CTDI_{vol}$	MSCT 25 mGy
ACR (2004)	Head	$CTDI_{w}$	60 mGy
	Abdomen		35 mGy
EC (1999)	Head	$CTDI_{w}$ and DLP	60 mGy, 1,050 mGy cm
	Chest		30 mGy, 650 mGy cm
	Abdomen/pelvis		35 mGy, 780 mGy cm

Source: NRPB (National Radiological Protection Board) (UK) (61); MSCT (European Concerted Action on CT) (71); ACR (American College of Radiology) (72); EC (European Commission) (23).

The Pediatric Patient

The ALARA principle is very important in pediatric applications. The activity of a radiopharmaceutical administered to a child is usually calculated by scaling down the adult dosage by the child's body weight or surface area (to maintain count density on planar imaging), subject to a minimum acceptable amount for very small children and infants (76, 77). Tumor-seeking radiopharmaceuticals used for imaging in pediatric oncology, radionuclide therapy, and for monitoring response to treatment have been summarized by Hoefnagel and de Kraker (78). Effective dose as a function of age for various radiopharmaceuticals is illustrated in Figure 4.3 (41, 73). Although the radiation dose is not the prime concern for these patients, FDG dose is clearly superior to ^{201}Tl-chloride or ^{67}Ga-citrate and is the radiopharmaceutical of choice for imaging, particularly when serial studies are indicated.

Pediatric CT factors are also required. As body size decreases and under the same exposure conditions, there is a marked increase in absorbed dose and the dose distribution from the periphery to the center becomes more uniform. It is important to reduce mA level to as few as 25 mAs for infants. Tube voltage should also be reduced for infants and small children to 100 kVp; at 80 kVp, an increase in beam hardening artifacts has been reported (79). For whole-body PET/CT scans, a protocol with a total beam width of 5 mm or more and a pitch greater than 1 is appropriate. Dose to children can be estimated using CT-Expo.xls phantoms for a 7-year-old and a baby, by applying scaling factors to the results calculated for adults using CTDosimetry.xls from v0.99r onward, or by using conversion factors at standard ages (0, 1, 5, and 10 years old) for DLP in various body regions (54, 55, 61).

Table 4.8. Effective dose from radionuclide imaging and diagnostic CT procedures.

		Protocol	mSv
Oncology[a]	^{18}F-FDG	370 MBq	7.0
	^{11}C-Methionine	400 MBq	2.1
	^{67}Ga-citrate	400 MBq	40.0
	^{201}Tl-chloride	120 MBq	19.2
	^{99m}Tc-mIBI	1 GBq	9.0
Brain[a]	^{15}O-water	1 GBq	0.93
	^{18}F-FDG	250 MBq	4.8
	^{99m}Tc-HMPAO	800 MBq	7.4
Myocardium[a]	^{13}N-Ammonia	550 MBq	1.1
	^{18}F-FDG	250 MBq	4.8
	^{99m}Tc-MIBI	1.3 GBq; 1-day rest/stress protocol	10.6
	^{201}Tl-chloride	140 MBq; stress/reinjection protocol	22.4
Bone[a]	^{18}F-NaF	250 MBq	6.0
	^{99m}Tc-MDP	800 MBq	4.6
CT[b]	Head	Acute stroke	1.7
	Chest	Lung cancer	6.9
	Abdomen	Liver metastases	7.1
	Abdomen/pelvis	Abscess	8.0
	Lung/abdomen/pelvis	Lymphoma survey, 636-mm length	12
CT in FDG PET/CT[c]	"Whole body" from neck to pelvis	Topogram Attenuation correction CT Diagnostic CT with contrast	0.2–0.4 1.3–4.5 14.1–18.6

[a]ICRP Publication 80 (41); data for ^{201}Tl from Thomas et al. (73).
[b]75th percentile doses from survey of CT practice in UK 2003; data from Shrimpton et al. (61).
[c]Data from survey of protocols at four centers by Brix et al. (75).

The Lactating Patient

PET studies with FDG for oncology or epilepsy investigations are infrequently requested for a woman who is breast-feeding an infant. Avid uptake of FDG in lactating breast tissue has been reported in a small series of patients (80). The uptake of FDG appears to be mediated by the GLUT-1 transporter, which is activated by suckling, not by prolactin. By imaging the breast before and after the expression of milk and counting the activity in milk samples, it was confirmed that FDG, being metabolically blocked, is not secreted in milk to any significant amount but is retained in glandular tissue. The dose to glandular tissue will be higher than the value for the nonlactating breast of 0.0117 mGy per MBq injected (81). The ^{18}F concentration in milk, measured in samples from one patient, was about 10 Bq mL^{-1} at 1 h and 5 Bq mL^{-1} at 3 h postinjection. It was postulated that the ^{18}F activity is associated with the cellular elements in milk, mainly lymphocytes. Using the standard model of breast-feeding with the first feed at 3 h postinjection (82), it was estimated that the dose to the infant from ingested milk would not exceed 85 μSv following an injection of up to 160 MBq FDG (and by

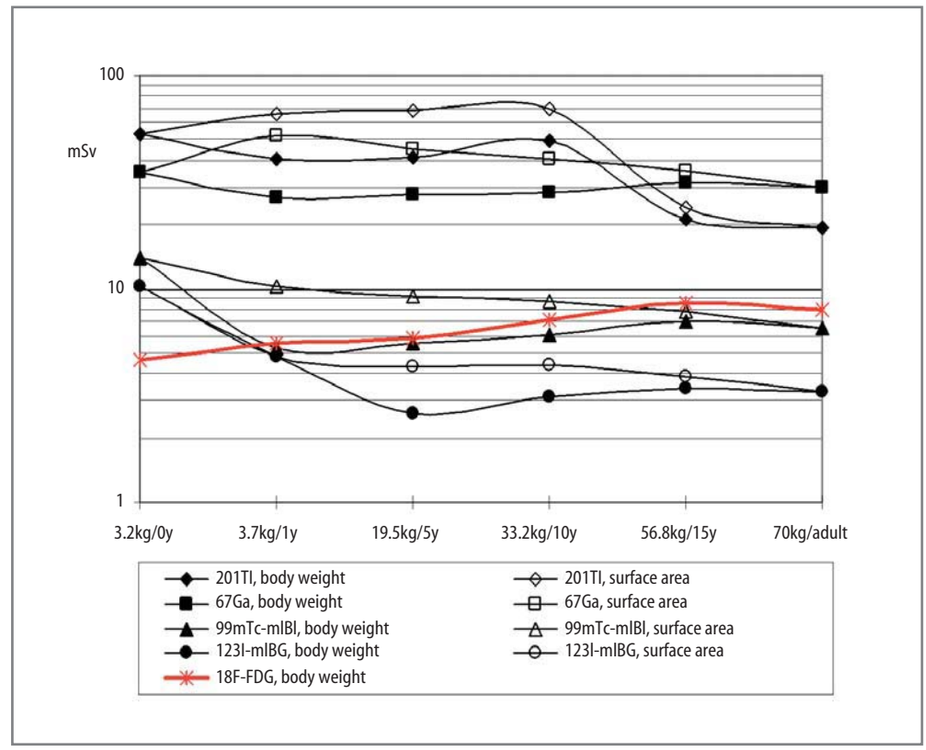

Figure 4.3. Dosimetry of radionuclide imaging in pediatric oncology. Administered activity scaled to adult dosage by body weight or surface area between limits of 20–120 MBq ^{201}Tl-chloride, 30–300 MBq ^{67}Ga-citrate, 100–720 MBq ^{99m}Tc-MIBI, and 70-250 MBq ^{123}I-MIBG, and by 6 MBq kg^{-1} body weight for ^{18}F-FDG (half this amount has been recommended for brain scans (107). Calculated from data in ICRP 80 (41) and Stabin (personal communication) for ^{18}F-FDG in newborn infants and for contaminant-free ^{201}Tl-chloride.

extrapolation up to 200 μSv after injection of 400 MBq). In addition, the infant would receive an external dose while being held while feeding from the breast or bottle. The dose rate against the chest could approach 200 μSv h^{-1} at 2 h after injection of 400 MBq FDG. Breast feeding and cuddling of the infant should be postponed for several hours after an FDG study if the infant's dose is to be kept below a dose constraint of 0.3 mSv for a single event (see following section).

The Pregnant Patient

Uterus dose from a diagnostic CT scan of the pelvis is typically about 30 to 40 mGy but could be considerably higher. One or two examinations of the abdomen/pelvis, for example, CT with and without contrast or followed by PET/CT, could cause the uterus dose to reach a level of 50 mGy, at which careful and individual fetal dosimetry assessment is recommended (83). In the zone between 100 and 500 mGy where adverse effects of radiation cannot be ruled out, the complex issues of risk and termination may be raised with the parents (12, 84). It is therefore understandable that the prospect of both CT and PET in a pregnant patient immediately raises concerns, especially if the pelvis will be in the field of view. The precautions used in radiology and nuclear medicine to discover before a scan if a female patient of childbearing capacity is or could be pregnant should be rigorously enforced in PET/CT to avoid the risk of inadvertent exposure of an embryo or fetus. If there is doubt about a pregnancy, a urine pregnancy test should be obtained or the scan postponed until after the next menstrual period.

The exposure of an embryo or fetus from a radiopharmaceutical depends on the biodistribution. In the earliest stages of pregnancy, dose to the embryo is taken to be the same as dose to the uterus. After about 12 weeks, when trophoblastic nutrition has been replaced by placental nutrition, fetal dose depends on whether the radiopharmaceutical or any of its metabolites accumulates in or is transferred across the placenta, as well as on the distribution of activity in the mother. Where placental transfer of radioactivity occurs, the activity is generally assumed to be distributed uniformly in the fetus. Fetal dose at various stages of gestation has been calculated for a range of radiopharmaceuticals using the MIRD methodology and an anatomic model of a pregnant female at 3, 6, and 9 months gestation, but at that time there was no documented evidence of placental transfer of FDG (85). Fetal uptake of FDG has since been imaged in humans (86, 87) and of FDG and ^{11}C-cocaine in nonhuman primates (37, 88). FDG dose coefficients at early pregnancy and at 3, 6, and 9 months gestation are now available for placental transfer and bladder voiding at 2-h and 4-h intervals (89). The shorter interval is more appropriate, as patients are generally instructed to empty the bladder within an hour of injection and to drink fluids after the scan. Iodide is also known to cross the placenta. The fetal thyroid begins to concentrate iodine from about the 13th week of pregnancy and reach a maximum concentration at about the

Table 4.9. Radiation dose to embryo/fetus from PET radiopharmaceuticals.

	Absorbed dose per unit activity administered to mother (mGy MBq−1)			
	Early	3 months	6 months	9 months
^{18}F-FDG, 2-h void[a]	0.018	0.018	0.016	0.015
^{18}F-FDG, 4-h void[a]	0.022	0.022	0.017	0.017
^{18}F-NaF[b]	0.022	0.017	0.0075	0.0068
^{124}I-NaI[b]	0.14	0.1	0.059	0.046
^{124}I-Na, fetal thyroid[c]	—	130	680	300

Source: Data from [a]Stabin (89), [b]Stabin (81), and [c]Watson (90).

5th to 6th month. Fetal thyroid dose from ^{124}I-NaI is included in Table 4.9 (81, 89, 90).

CT dose to an embryo or fetus in early stages of pregnancy is assumed to be the same as the dose to the uterus, which can be estimated with CT dose calculation software. If the uterus is not in the scanned region, the dose falls off exponentially beyond 3 cm from the scan limit. In an early method of estimating dose to the fetus from CT, whether in the primary beam or outside the scanned region, correction factors at 1cm intervals from the fetal midpoint to the upper and lower scan limits were applied to the $CTDI_{100}$ (in the head phantom) for the same conditions of exposure including slice thickness and pitch (91). Monte Carlo simulation has been used to assess dose within and beyond the scanned region, from which look-up tables of dose normalized to 100 mAs at various kVp and beam shaping filters were prepared (92). In mid- to late pregnancy, when the body cross section more closely approximates a circle, the $CTDI_{vol}$ in the 32-cm body phantom at the appropriate kVp should give a reasonable indication of fetal dose.

It is important to use low-dose CT protocols when PET/CT scanning is indicated in a pregnant patient whose condition allows for the possibility of fetal survival. The protocols should be established in advance. For whole-body oncology studies, the fetus is exposed during both PET and CT components. For brain and cardiac studies, fetal exposure is almost entirely caused by the PET radiopharmaceutical. Depending on the PET/CT scanner characteristics and the stage of pregnancy, it is possible to limit fetal dose from a whole-body scan to less than 15 mGy (350 MBq FDG injection, 120 kVp CT beam 10 mm wide, pitch of 1.5 and 80 mAs) and from a brain scan to less than 4 mGy (from 250 MBq FDG and negligible dose from CT) (Figure 4.4) (86). If the usual injected activity of FDG is reduced, scan time should be scaled up to maintain sensitivity for detection of small lesions. These fetal doses are below the threshold for radiation-induced abnormalities, would have minimal effect (about 1 in 1,000 or less) on the incidence of fatal cancer in childhood, and would not increase the normal risks of pregnancy.

The Volunteer Exposed for Medical Research

One area in which dose estimates are required is the recruitment of volunteers to participate in research studies. Regulatory authorities in many countries have adopted the recommendations of the ICRP (93): an exposure for research purposes is treated on the same basis as a medical exposure and therefore is not subject to a specific

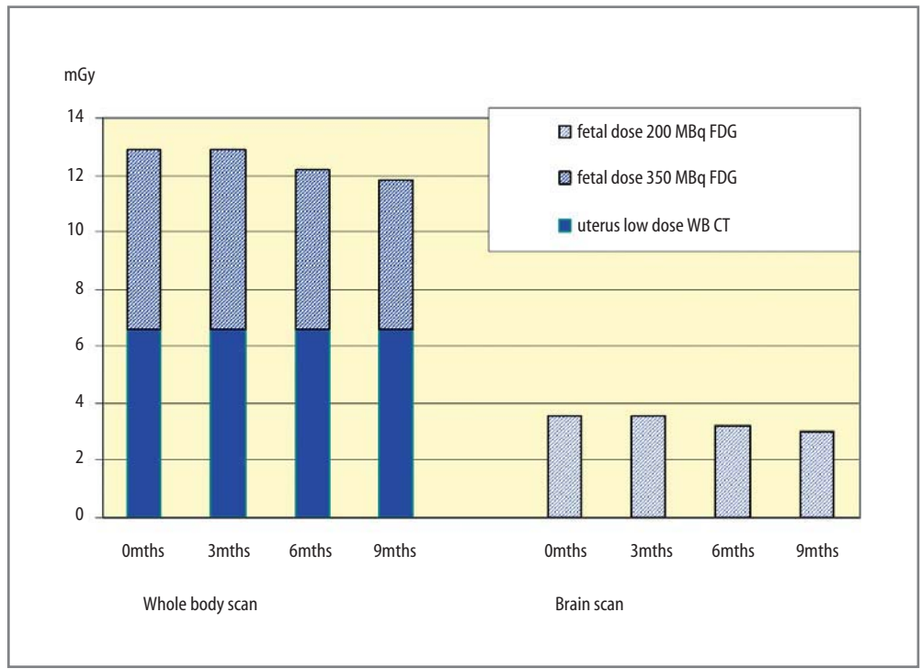

Figure 4.4. Fetal dose estimates for optimized low-dose FDG PET/CT whole-body and brain scan protocols in pregnancy. Calculated for FDG placental crossover and 2-h bladder voiding interval (89); CT whole-body scan Siemens Biograph, 110 kVp, 113 mA, 0.8-s rotation, 2 x 5 mm beam width, pitch 1.5 (55).

dose limit, the dose should be commensurate with the potential benefit of the research findings, and the study protocol should be approved by a properly constituted ethics committee. A constraint on effective dose may apply where the participant is not expected to benefit from the exposure, as in the exposure of "normal" subjects or patients enrolled in a clinical trial that involves additional or different exposures to what would otherwise be required for clinical management. The dose constraint would be considered, for example, in determining the maximum number of injections of ^{15}O-water for repeated tests of cognitive function in normal volunteers. It is unlikely that PET/CT research studies would fall below a dose constraint as low as 5 mSv, and these protocols may require further consideration by a regulatory authority or similar agency. The ICRP has published "realistic maximum" dose coefficients for ^{11}C-labeled substances and generic dose coefficients for ^{11}C- or ^{18}F-labeled amino acids and ^{11}C-brain receptor ligands, which are useful when preparing research submissions involving novel agents for which dosimetry data in humans are not yet available (43).

Occupational and Public Exposures

Health Care Workers Within and Outside the PET Facility

It has been known for many years that the radiation exposure to a technologist performing PET studies is generally higher than for conventional nuclear medicine imaging (94–96). Substantial shielding of syringes, vials, and transmission and quality control sources is standard practice in PET facilities. With inanimate sources effectively shielded, attention has turned to minimizing the exposure to staff from patients. Education of staff on the importance of distance and time is a key factor in dose control (97–100); see also Chapter 3. If operators need to be cross-trained to perform PET/CT procedures, it may be more of a challenge for a radiographer to adapt to handling unsealed sources and "hot" patients and receiving an occupational exposure of several mSv per year, than for a nuclear medicine technologist to prepare patients for a CT scan, follow preset CT protocols, and observe CT radiation safety precautions.

The dose to employees is likely to increase as PET/CT systems proliferate and it becomes feasible to scan 20 patients on one system in a day. In particular, employees who work in mobile PET/CT units may receive higher exposures because of space constraints and less opportunity to share duties requiring close contact with patients. Employee doses reported from different PET facilities are difficult to compare because of the variability in isotope supply, clinical workload, scan protocols, and physical accommodation. Surveys are most useful if quoted in terms of dose per GBq handled or per procedure stating the injected activity. With due care and some rostering (say 50%) with other nuclear medicine duties, it should be possible to keep employee dose at or below 5 mSv year^{-1} while scanning up to 20 PET patients per day.

Task-specific monitoring can be used to identify actions that contribute most to staff exposure and to suggest areas for improvement (101–104). The most significant contribution to dose occurs during close contact with the patient, as is to be expected because vials and syringes can be shielded but dose rates within 0.5 m of the patient can be of the order of 4 to 8 μSv min^{-1} following an injection of FDG. Dose rates near the FDG patient have been measured in a number of studies, at different orientations to the patient, and at different times postinjection (95, 96, 99, 100, 105, 106). Representative values are shown in Table 4.10. From such data, the American Association of Physicists in Medicine (AAPM) proposes a mean normalized dose rate of 92 μSv GBq^{-1} h^{-1} at 1 m in any direction from the patient for radiation protection planning (see following). This value would also be applicable for other PET nuclides with no other gamma emissions after correcting for the branching ratio. An example of the pattern of exposure from individual tasks involving contact with patients is shown in Figure 4.5. Dose rates can be integrated to give an indication of dose per task as shown in Figure 4.6, which if normalized to the radionuclide activity can be used for comparison between tasks, individuals, and facilities.

Close attention should be given to strategies that eliminate, postpone, or shorten time in close contact with the patient. Important measures include explaining the procedure, pointing out where the patient will go, administering medications, setting up EEGs, and establishing intravenous access by cannula with a saline flush syringe on a three-way tap or with an infusion set before administering the dose; flushing the dose immediately from the line, postponing the removal of lines and catheters until the conclusion of scanning, and using a tourniquet or asking the patient to maintain pressure on the puncture site after removal of a line; keeping at a distance while

Table 4.10. External dose rates near FDG patients.

Patient position, measurement location	Distance (m)	Normalized dose rate (95th percentiles) (μSv h^{-1} per MBq injected)	
		Postinjection[a]	2 h post injection[b]
Standing, at anterior chest	0.5	0.60	0.20
	2.0	0.10	0.03
Supine, at side	0.5	0.85	—
	2.0	0.11	—
Supine, at head	0.5	0.36	—
	2.0	0.075	—
Supine, at feet	0.5	0.078	—
	2.0	0.023	—

Source: Data from [a]Benatar et al. (105) and [b]Cronin et al. (106).

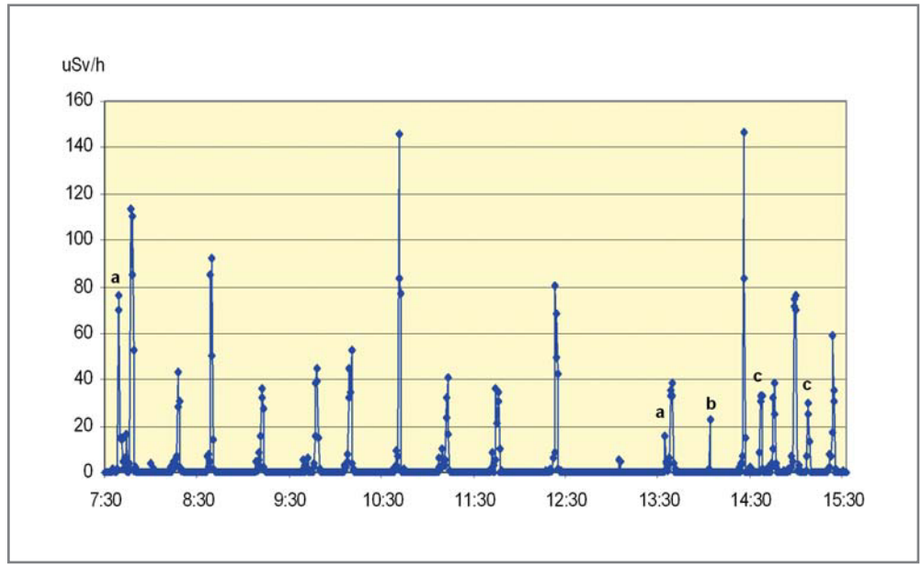

Figure 4.5. Exposure to a positron emission tomography (PET) technologist throughout the day. *Unlabeled peaks:* dispense–calibrate–inject 350 MBq ^{18}F-FDG for 15 patients. Dose rates are generally less than 60 μSv h^{-1} although can be as high as 150 μSv h^{-1} depending on proximity to the injection site. *Other peaks:* (**a**) unpacking two FDG deliveries; (**b**) directing a patient to toilet; (**c**) taking two blood samples. (Royal Prince Alfred Hospital, measurements with Eberline FH 41B-10 system; courtesy of R. Smart.)

directing patients to the toilet, using a wheelchair to move frail patients to and from the scanner as quickly as possible, and enlisting other persons to assist with patient handling. Nurses working within hospital PET facilities that scan many high-dependency patients may be the "critical group" so far as staff exposure is concerned. Specific practices are recommended for pediatric patients (107, 108). The quantitative measurement of cerebral glucose metabolism originally required a number of blood samples to be taken over a period of 30 to 40 min following the injection of FDG, resulting in significant operator exposure (109). A two-sample method has been developed with a fivefold reduction in operator dose per study (110).

Hand doses in PET may also be higher than in conventional nuclear medicine and are strongly influenced by technique because the radiation fields around partially shielded syringes and vials are highly directional. The report of a detailed study using thermoluminescent dosimeters (TLD) to measure dose to the hands during dispensing of FDG injections contains information that could be extrapolated to other facilities (111). The skin dose [H′(0.07)] measured at 18 locations on each hand ranged from about 100 to 300 μSv per GBq dispensed. The dose was higher on the nondominant hand. The dose at the base of the middle finger, a preferred position for wearing a ring dosimeter, was close to the average for the hand

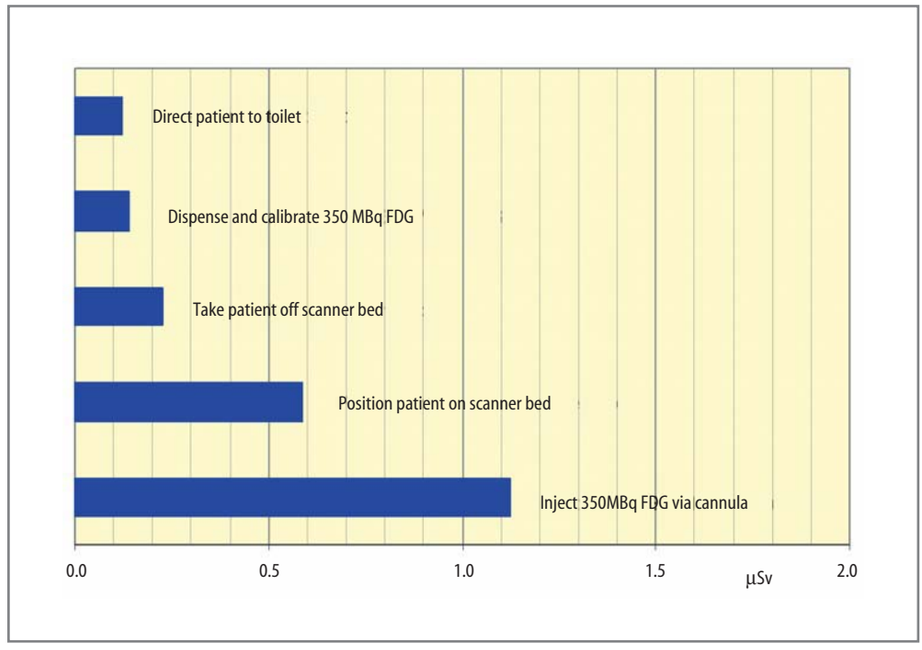

Figure 4.6. Dose to PET technologists performing specific tasks. (Royal Prince Alfred Hospital, measurements with Eberline FH 41B-10 dosemeter.)

and about half of the maximum dose location for the hand. The use of a tungsten syringe shield or an automated dispenser did not provide the expected improvement in protection because of the additional handling to remove the syringe shield to calibrate the filled syringe or to remove a filled syringe from the dispenser.

The duties and previous personal dosimetry history of an employee who declares that she is pregnant and wishes to continue at work during the pregnancy should be reviewed. The ICRP recommends that the fetus should be afforded the same level of protection as a member of the public (4) and has suggested that the use of shielding and/or isolation of sources in the workplace usually provides an adequate level of protection without the need for specific restrictions on the employment of pregnant women (3). However, this is not always possible in a PET workplace, and restrictions on the contact a pregnant employee has with patients are likely to be needed.

Following a PET scan, the patient may come into close contact with other health professionals. Dose rate measurements at various distances from the patient on leaving the PET facility, combined with modeling of potential patterns of close contact, indicated that nurses on a ward that regularly sends patients for PET scans are unlikely to receive more than 24 μSv per day (106). The exposure rate to a sonographer working at 0.5 m from a patient who received 400 MBq FDG 2 h prior would be about 40 μSv h^{-1} (112). In circumstances where a staff member may have frequent contact with PET patients, for example, nursing staff or porters of an oncology ward, personal dosimeters can be used to establish the level of exposure for informed guidance on policies and procedures. In most cases, contact is so infrequent that no special precautions are required.

Family Members, Carers, and Members of the Public

The dose limit of 1 mSv $year^{-1}$ for members of the public recommended by the ICRP has been widely adopted. This limit is used as a criterion when discharging radionuclide therapy patients from hospital, although a dose constraint of 0.3 mSv from any single event has subsequently been proposed (by the European Union) to allow for several exposures occurring during the course of a year (113). The dose to persons near a PET patient depends on the activity in the patient and excretion (if any), and the pattern of close contact effectively within a distance of about 2 m or less. Only ^{18}F sources need be considered. The dose to persons near a patient has been modeled for a number of scenarios, showing there is no need to restrict the activities of patients for the remainder of the day of their PET scan to satisfy a dose constraint of 0.3 mSv per event (106).

Persons knowingly and willingly assisting with the support of the patient are regarded by the ICRP as carers, not subject to the dose limit for members of the public. A dose constraint of 5 mSv per event has been proposed for carers (113]. Other family members—especially children—should be subject to the same dose constraint as members of the public, as it is quite possible that the patient will undergo more than one radionuclide imaging procedure within a year. Not all the accompanying persons in a common waiting area of a PET facility may qualify as carers. For them, the 0.3-mSv dose constraint may be exceeded if they are seated among patients who have been injected with FDG and are waiting to be scanned. Patients should be advised at the time of booking that they should not be accompanied by pregnant women, infants, or children when attending for the scan. If this cannot be arranged, the accompanying persons should neither stay with the patient during the FDG uptake phase nor wait in an area used by other injected patients.

Facilities and Equipment

Facility Planning for Radiation Protection

The main impact of PET/CT on radiation safety is a significant increase in clinical workload that has implications for the layout and shielding of the whole facility. The scanner room is likely to be the busiest point of a facility. Injected patients are a mobile and significant source of exposure, so isolation and internal traffic are important aspects of facility planning. The layout should minimize the distance to escort patients between preparation rooms, toilets, scanner room, and postscan waiting areas and also avoid incidental contacts between patients in transit and other staff. Generously sized change cubicles, toilet areas, and preparation rooms, trolley bays with ready access to the scanner room, and handrails and support aids will reduce staff exposure while assisting frail patients moving to and from the scanner, toileting, or dressing. The scanner design and location should allow a patient to get on and off the scanner bed with minimal assistance, or to be transferred quickly to and from a trolley if necessary. A “cold” waiting area should be available for patients before injection and for accompanying persons. With a capacity of up to 20 FDG scans a day, a single PET/CT scanner could require three patient preparation areas for FDG injection and uptake. A single preparation area shared by all patients is not recommended as it would unnecessarily increase the exposure of the person giving the injections. Space may have to be found within the limits of an existing facility, remembering that other imaging and counting equipment should be separated or shielded to prevent interference from patients and syringes.

Shielding

The scanner room, preparation rooms, and possibly a postscan waiting area may need substantial shielding

depending on the degree of isolation from occupied areas and other imaging and counting equipment. Professional organizations such as the AAPM may be consulted for authoritative information on design and shielding issues. PET radionuclides present more of a challenge than other radionuclides used for diagnostic imaging in nuclear medicine, or diagnostic X-rays for that matter, because of their higher photon energy and hence smaller cross section for photoelectric absorption. The objective of shielding design is to determine the transmission ratio (B) of dose rates, or of dose integrated over a specified interval, with and without the shield in place. The thickness of shielding material to achieve the desired value of B can then be calculated or obtained from published data.

Small sources in the workplace or during transport should be shielded to attenuate the maximum dose rate intensity to an acceptable value ($B = I/I_0$) at a nominal close distance, say less than 10 μSv h^{-1} at 0.3 m, or as specified in Transport codes. Dose rates at the distance of interest can be calculated from the rate constants in Table 4.4. The appropriate quantity to use for operational purposes is the ambient dose equivalent [H*(10)] or deep dose equivalent (DDE), which is the dose at 10-mm depth in tissue, rather than air kerma (114, 115). This criterion allows a small margin of safety above the effective dose E (or effective dose equivalent EDE or H_E) in which dose limits are defined using tissue weighting factors of various vintage, but which cannot be measured "in principle or in practice". If necessary, factors are available to convert from air kerma to H*(10) and E (116) or DDE and EDE (117).

Vials and syringes are treated as point sources, with the dose rate being inversely related to the square of the distance from the source. The dose rate at a distance from a line source can be calculated by the appropriate formula (118, 119). The values in Table 4.5 of mean half- and tenth-value layers (HVL and TVL) are suitable for estimating shield thickness in high-density materials such as lead and tungsten. Lead thickness in a clinical PET setting is typically 50 mm for bench shields, storage caves for waste, and PET camera quality control sources, 30 mm for vial containers located behind a bench shield, and 15 mm for syringe shields. The lead glass for a window in a bench shield has superior optical transmission if supplied as a single piece rather than stacked sheets. Vial and syringe shields are too heavy to manipulate with safety so mechanical supports are necessary when dispensing and injecting PET radiopharmaceuticals. Tungsten may be preferable to lead for small PET source containers. For example, a cylindrical pot for a vial 5 cm high and 2 cm in diameter designed for 1% transmission (two tenth-value layers) would be approximately 25% heavier and 30% wider if fabricated in lead rather than tungsten.

Plastic liners may be used within lead or tungsten vial and syringe shields to absorb all positrons, although most positrons from ^{18}F would be absorbed in the vial or syringe wall. ^{15}O positrons absorbed in lead could generate bremsstrahlung (X-ray) photons up to their maximum energy of 1.7 MeV. However the energy converted to bremsstrahlung radiation is a small fraction of the average positron energy incident on a lead or tungsten shield (from less than 2% in the case of ^{18}F to 5% in the case of ^{11}C). The practical value of plastic syringe shield inserts is to increase the distance of the fingers from the source and possibly screen the skin from longer-range positrons.

Rooms used by "hot" patients generally require shielding. The room used for storing and dispensing PET radiopharmaceuticals and storing transmission/QC sources may also need some shielding to supplement source containers. A conservative approach to shielding design may avoid the need for expensive retrofits as technology improves but must be balanced against the cost (expense and space) of the safety margin, which could be considerably more in PET than in radiology. A reasonable estimate of future workload is needed for both PET and CT in terms of number of patients, type of study, and protocol. With the advent of PET/CT, the number of patients scanned in a day is limited more by the time for patient handling, including changeover, positioning, and clinical purposes such as administration of contrast or markup for radiation therapy, than by the time for the transmission scan.

A similar design method can be used for X-ray and PET sources (120–122). Barriers between the source and an occupied area should attenuate the dose D_0 without shielding for the maximum anticipated workload during a specified interval, usually 1 week, to an acceptable design limit D ($B = D/D_0$). The value of D depends on who has access to the area in question, and for how long. Regulatory authorities should be consulted for local requirements. The limit may be adjusted for partial occupancy of the area by individuals while the source is present, normally taken to be a 40-h working week. By convention, full-time occupancy is assumed for "controlled" work areas, and the regulatory design limit for these areas could be as high as 100 or 120 μSv per week (96). However, because PET staff must also have close contact with radioactive patients, for example, about 30 min per day at centers scanning up to 10 patients per day (105, 123), their exposure at all other times should be kept as low as reasonably achievable by designing barriers to 20 μSv or less in a week, particularly for the control room where they spend a lot of time. A low level of ambient radiation in the workplace is reassuring when recruiting staff and reduces the need for rostering to meet dose constraints. For areas to which the public has access, the design limit is usually 20 μSv per week or a lesser dose constraint. Default values for occupancy factors (T= 1) recommended by the NCRP or other bodies for public areas (120) can be used if the anticipated use of the area does not allow a firm estimate of occupancy.

The unshielded dose (D_0) at a specified distance can be determined from the workload (W) expressed as GBq-h per week for radionuclides or mA-min per week for head and body scans at specified kVp for X-ray apparatus. PET

workloads for each room are determined by the activity injected and excreted, the number of patients, and the time of entry and exit to the room. W, the activity-time integral in each room, should allow for radioactive decay and excretion losses before the patient's entry and radioactive decay while in the room. A reasonably conservative approach would be to assume a high throughput of patients and injected activity based on the scanner specifications and the experience of busy centers. Currently, about 90% of patients undergo oncology (whole-body) studies, being scanned from 45 to 90 min after injection of 150 to 800 MBq FDG. Immediately before the scan, the patient is asked to empty the bladder, removing about 10% to 20% of the injected activity that has been excreted in urine. Scan time can range from 15 to 45 minutes or more. The remaining 10% of patients generally undergo brain or cardiac studies of shorter duration. The daily pattern of unshielded dose rate in a PET/CT scanner room is illustrated in Figure 4.7.

D_0 is calculated from the product of W and the dose rate at 1 m from the patient, corrected for distance. The dose rate constants for a point source are not applicable for an extended source geometry and do not allow for self-attenuation in the source. A mean dose rate of 92 μSv h^{-1} per GBq at 1 m in any direction from an FDG patient, based on measurements reported in the literature, is proposed by the AAPM (D. Simpkin, personal communication). No allowance is made for attenuation of 511 keV in the scanner gantry or other hardware, which is a very conservative assumption. When calculating distance, the patient is regarded as a point source located 1 m above the floor, at the midpoint of the scan range or on the bed or chair used during the uptake phase. The point of occupation is taken to be 0.5 m beyond a wall, 0.5 m above the floor level above, or 1.7 m above the floor level below. The inverse square law is generally used to adjust the dose for distance. Except for the scanner room itself, room dimensions and distances to the nearest occupied areas may be small, as in a mobile trailer facility. At close range (less than 3 m), an inverse 1.5 power of the distance is more appropriate. For example, to reduce the dose from a workload of 12 GBq-h per week to 20 μSv at 2 m or 4 m, the required B would be $20/(12 \times 92/2^{1.5}) = 0.05$ or $20/(12 \times 92/4^2) = 0.29$, respectively.

The upper limit on the estimate of CT workload would be to assume the system is used for diagnostic CT only (for example, if isotope supply were interrupted) with more patients and higher exposure factors, for example, 200 patients and 40,000 mA-min per week. It may be more realistic to assume the same number of patients as for the PET workload and diagnostic or non-diagnostic CT protocols as per local policy. The primary CT beam is absorbed in the patient or scanner, leaving only leakage and scattered radiation, which is of short duration and substantially lower energy than 511 keV, to consider. The unshielded dose can be estimated from the workload and isodose contours or a scatter distribution grid map (dose per unit workload) supplied by the manufacturer.

The thickness of a barrier for the required value of B can be determined from half- and tenth-value layers or published transmission curves. Under idealized "narrow beam" conditions with scatter excluded by collimation of the source and detector, the attenuation of a monochro-

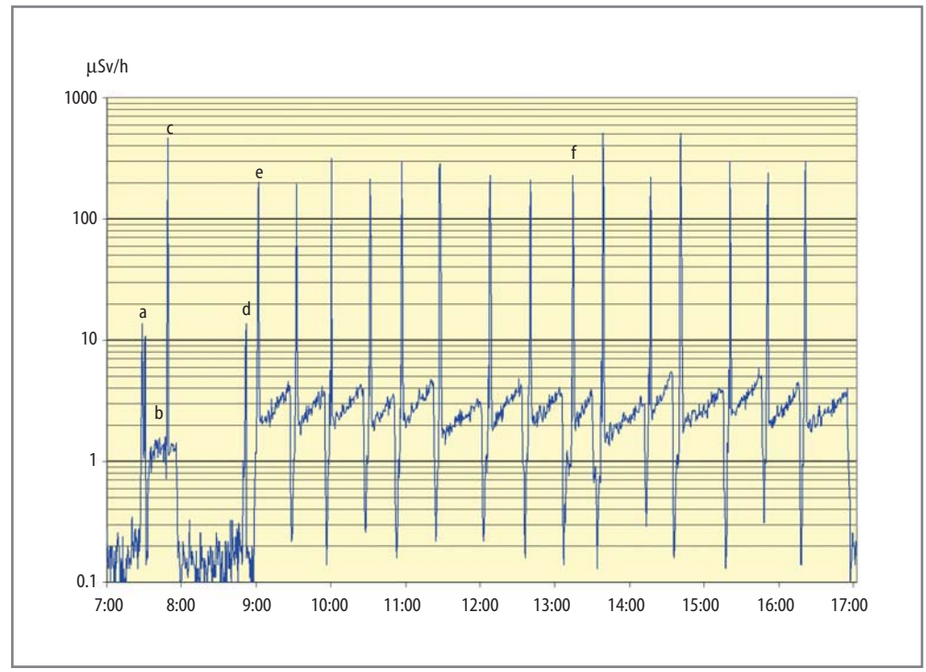

Figure 4.7. Pattern of exposure on wall at head end of Siemens Biograph scanner throughout the day. Dose rates: (**a**) CT warm-up and calibration; (**b**) PET phantom quality control; (**c**) CT during PET/CT acquisition with PET phantom; (**d**) CT calibration; (**e**) CT for 1 of 12 whole-body scans; (**f**) CT for one of three brain scans. During PET acquisitions, ^{18}F dose rate rises as scanner bed moves through the gantry toward the wall. PET and CT radiation detected at 1-m height, 2.1 m from isocenter with Eberline FH 41B-10.

matic beam of radiation through an absorbing medium is described by the following equation:

$$I = I_0 e^{-\mu x}$$

In this case, B is a simple exponential attenuation factor and μ is the linear attenuation coefficient at a given energy for the shielding material concerned. The thickness (x) of the shield for a given energy and material would be calculated from known values of μ, or of the total mass attenuation coefficient μ/ρ and the density ρ (118, 119). However a simple exponential function is not suitable for the "broad beam" geometry of extended radionuclide sources with energies of more than a few hundred keV and barrier materials of low atomic number in which Compton scattering is the predominant interaction, as for 511-keV PET photons incident on concrete barriers. Under broad beam conditions, scatter in the forward direction builds up in the barrier until an equilibrium depth is reached beyond which attenuation is more nearly exponential. Broad beam transmission can be estimated by point kernel or Monte Carlo modeling. Alternatively, the half- and tenth-value layers given in Table 4.5 can be used as they apply to broad beam conditions and moderate B values, not being derived from μ for narrow beams or from an average attenuation over many orders of magnitude as in NCRP Report No. 49 (19, 20, 124). The various estimates of transmission of 511-keV photons through lead and concrete are shown in Figure 4.8, indicating how narrow beam analysis significantly underestimates transmission through concrete (20, 118, 125).

PET barriers around patients generally require modest attenuation with B of the order of 0.1 to 0.4, but this can translate to substantial thickness of lead or concrete. In marked contrast, typical values of B for a CT installation are in the range of 10^{-3} to 10^{-4}. Transmission curves in lead and concrete for CT secondary radiation (scatter and leakage) at various kVp calculated by Simpkin are available (120, 122, 126). Attenuation is not a single exponential function because the beam is not monoenergetic. The final slope represents the attenuation coefficient for the highest energies, as from leakage radiation. The thickness of lead required for CT installations is generally less than 2 mm, which has little effect on 511-keV photons, whereas the thickness of concrete may be similar for PET and CT requirements. Figure 4.9 illustrates the attenuation through barriers of lead or concrete for a notional weekly workload of 100 patients injected with 500 MBq FDG for whole-body scans using low-dose CT protocols. It is necessary to consider PET and CT workloads and transmission independently and estimate the contribution of each to the total dose for various barrier material options.

Cost factors apart, lead has the advantage over concrete for walls because it requires less space and reduces the floor loading by roughly half. A combination of the two may be an effective solution. It is preferable to position the doors to the scanner room where shielding is required for CT only. All the doors to the scanner room should have the usual radiation warning sign and light for CT and should not be interlocked to the operation of the scanner. Depending on the view of the regulatory authority, it may be possible to avoid the considerable expense of a large leaded glass viewing window to the control room, or at least minimize the size of the window, by using video camera surveillance to give the technologist a clear view of

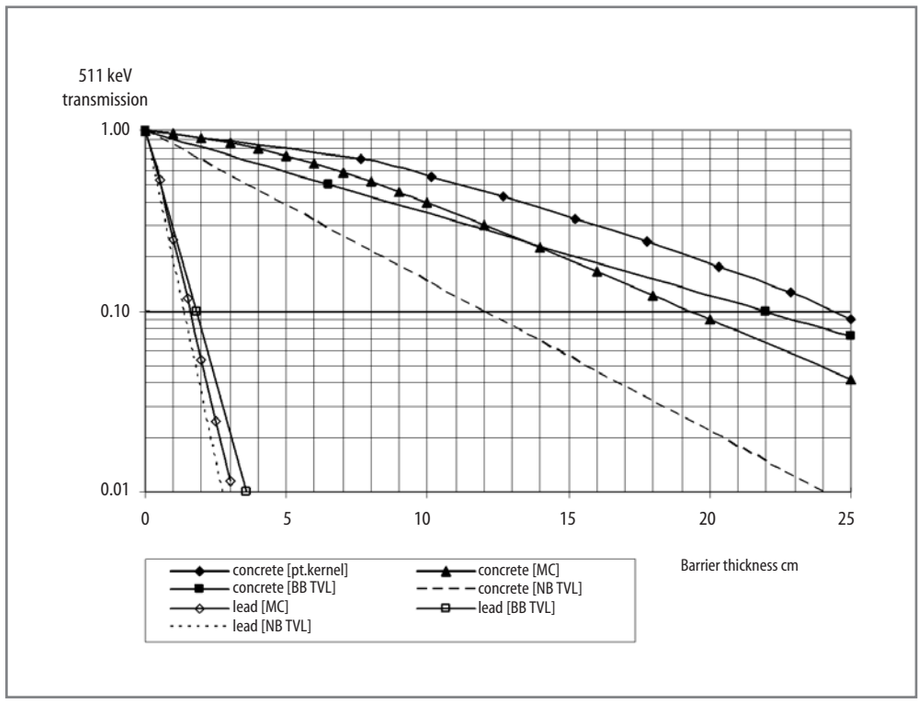

Figure 4.8. Attenuation of 511-keV photons in concrete (2.2 g cm^{-3}) and lead, calculated by Monte Carlo and point kernel modeling (125); Simpkin and Courtney, personal communications) and from broad and narrow beam linear attenuation coefficients (20, 118).

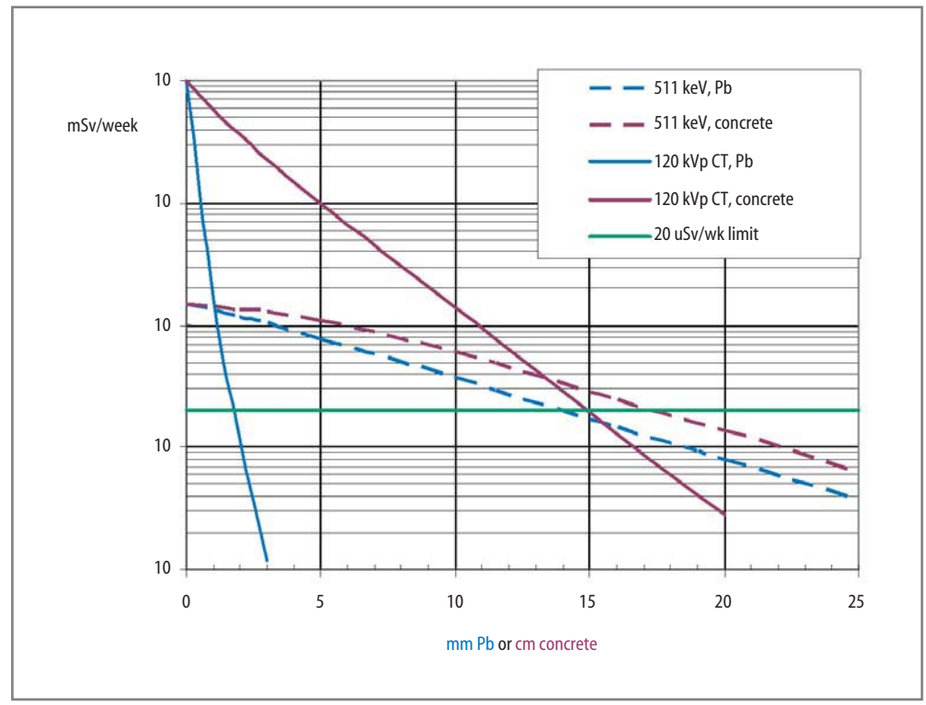

Figure 4.9. Shielding estimation for area adjacent to a PET/CT scanner that receives 0.15 mSv from ^{18}F and 10 mSv from 120-kVp CT secondary radiation in a week from notional workload of 100 patients injected with 500 MBq ^{18}F-FDG.

the patient and entry doors. If not, it is important that the attenuation properties of the window are specified at 511 keV as well as for the X-rays. The linear attenuation coefficient of leaded glass is the sum of the linear attenuation coefficients for lead and glass in the mixture, which can be calculated from their respective mass attenuation coefficients and their densities in the mixture if the percentages by weight are known (127). For example, a window of glass that is 55% lead by weight and 1.4 cm thick would have a transmission B of about 0.62, allowing for buildup (P. Brown, personal communication).

Containment of Sources

Spills are an uncommon event and usually result from mishaps with intravenous lines or urinary catheters. Strategically located dispensers for disposable gloves are convenient when dealing with radiopharmaceuticals, patients, and waste. The importance of gloves and monitoring can be seen from the dose rates for skin contamination in Table 4.5: a droplet from an FDG solution with a concentration of 100 MBq mL^{-1} could deliver 500 mSv, the annual dose limit for the skin, in just 6 min.

In facilities located near a cyclotron, PET gas tracers may be used. The gas supply and return lines from the radiochemistry laboratory to the scanner room will require shielding; the scanner manufacturer may specify an allowable maximum dose rate adjacent to the gantry. In occupied areas and the PET scanner room itself, a thickness of 20 to 25 mm of lead around the lines may be sufficient. A mask over the patient's head should effectively contain the administered gas and scavenge the exhaled gas for venting via a stack to the atmosphere. The air of the PET scanner room should be continuously monitored during a gas study. Because of the high background radiation level in the room, an air sampler is required to pass the air through a sensitive detector in a remote low-background area. The scanner room should be kept at negative pressure to the adjacent areas. The room air should not be recirculated but vented direct to atmosphere.

Radiation Instrumentation

The dose calibrator used in general nuclear medicine applications is adequate for PET in a clinical setting. A high ranging chamber may be required in a PET production laboratory if measuring very high activities. The chamber should be provided with additional shielding, up to 50 mm of lead, to protect the operator during PET nuclide measurements. With 511-keV photons, no corrections should be required for the geometry of the source container (e.g., syringe, vial) or volume; the manufacturer's settings possibly overestimate the activity of ^{18}F by 3% to 6% depending on the geometry (128).

Radiation instrumentation should include a survey meter, preferably a dual-purpose instrument for measurement of dose rate and surface contamination. Geiger-Mueller (GM) detectors have good sensitivity to PET nuclide emissions, and their energy response is fairly uniform over the photon energy range of a few hundred keV. No energy response correction is necessary for a GM meter that has been calibrated at 660 keV with a ^{137}Cs

source. Finally, an electronic personal dosimeter is a very useful investment for monitoring staff in training or performing tasks where dose rates are high or there is prolonged close contact with a source.

References

1. Beyer T, Antoch G, Muller S, et al. Acquisition protocol considerations for combined PET/CT imaging. J Nucl Med 2004;45:25S–35S.
2. Antoch G, Freudenberg L, Beyer T, et al. To enhance or not enhance? 18F-FDG and CT contrast agents in dual-modality 18F-FDG PET/CT. J Nucl Med 2004;45:56S–65S.
3. International Commission on Radiological Protection. 1990 Recommendations of the International Commission on Radiological Protection. ICRP Publication 60. Oxford: Pergamon, 1991.
4. International Commission on Radiological Protection. ICRP 2005 Draft Recommendations: www.icrp.org; 2005.
5. United Nations Scientific Committee on the Effects of Atomic Radiation. Sources and effects of ionizing radiation. Vol 1: Sources. UNSCEAR 2000 Report. UNSCEAR, 2000.
6. Preston D, Pierce D, Shimizu Y, et al. Dose response and temporal patterns of radiation-associated solid cancer risks. Health Phys 2003;85:43–46.
7. Ron E. Cancer risks from medical radiation. Health Phys 2003;85:47–59.
8. National Radiological Protection Board. Board Statement on Diagnostic Medical Exposures to Ionising Radiation During Pregnancy and Estimates of Late Radiation Risks to the UK Population. Chilton: NRPB, 1993.
9. Brenner DJ, Elliston CD, Hall EJ, et al. Estimated risks of radiation-induced fatal cancers from pediatric CT. AJR 2001;176:289–296.
10. Donnelly LF, Emery KH, Brody AS, et al. Minimizing radiation dose for pediatric body applications of the single-detector helical CT: strategies at a large children's hospital. AJR 2001;176:303–306.
11. Paterson A, Frush DP, Donnelly LF. Helical CT of the body: are settings adjusted for pediatric patients? AJR 2001;176:297–301.
12. International Commission on Radiological Protection. Pregnancy and Medical Radiation. ICRP Publication 84. Oxford: Pergamon, 2000.
13. Lowe SA. Diagnostic radiography in pregnancy: risks and reality. ANZJOG 2004;44:191–196.
14. Wakeford R, Little MP. Childhood cancer after low-level intrauterine exposure to radiation. J Radiol Prot 2002;22:A123–A127.
15. Doll R WR. Risk of childhood cancer from fetal irradiation. Br J Radiol 1997;70:130–139.
16. Dillman LT. Radionuclide decay schemes and nuclear parameters for use in radiation-dose estimation. MIRD Pamphlet No. 4. J Nucl Med 1969;10(suppl 2).
17. Dillman LT. Radionuclide decay schemes and nuclear parameters for use in radiation-dose estimation, Part 2. MIRD Pamphlet No. 6. J Nucl Med 1969;11(suppl 4).
18. Groenewald W, Wasserman H. Constants for calculating ambient and directional dose equivalents from radionuclide point sources. Health Phys 1990;58:655–658.
19. Delacroix D, Guerre JP, Leblanc P, et al. Radionuclide and Radiation Protection Handbook 1998. Radiat Prot Dosim 1998;76.
20. Wachsmann F, Drexler G. Graphs and Tables for Use in Radiology. Berlin: Springer-Verlag, 1976.
21. Seibert JA. X-ray imaging physics for nuclear medicine technologists. Part 1: Basic principles of X-ray production. J Nucl Med Technol 2004;32:139–147.
22. International Commission on Radiological Protection. Managing Patient Dose in Computed Tomography. ICRP Publication 87. Oxford: Pergamon, 2000.
23. European Commission. Report No. EUR 16262 EN. European Guidelines on Quality Criteria for Computed Tomography, 1999.
24. Rizzo SMR, Kalra MK, Maher MM, et al. Do metallic endoprostheses increase radiation dose associated with automatic tube-current modulation in abdominal-pelvic MDCT? A phantom and patient study. AJR 2005;184:491–496.
25. Keat N. CT scanner automatic exposure control systems. Report No. 05016. ImPACT CT Scanner Evaluation Centre, 2005.
26. Britten A, Crotty M, Kiremidjian H, et al. The addition of computer simulated noise to investigate radiation dose and image quality in images with spatial correlation of statistical noise: an example application to X-ray CT of the brain. Br J Radiol 2004;77:323–328.
27. Platten D, Keat N, Lewis MH, et al. Sixteen slice CT scanner comparison report. Report No. 05013. Version 12. ImPACT CT Scanner Evaluation Centre, 2005.
28. Nagel HD, editor. Radiation Exposure in Computed Tomography, 4th ed. Hamburg: CTB Publications, 2002.
29. Watson CC, Casey M, Beyer T, et al. Evaluation of clinical PET count rate performance. IEEE Trans Nucl Sci 2003;50:1379–1385.
30. Watson CC, Casey ME, Bendriem B, et al. Optimizing injected dose in clinical PET imaging by accurately modeling the count rate response functions specific to individual patient scans. J Nucl Med 2005;46(11):1825–1834.
31. Eberl S, Fulham MJ, Meikle SR et al. Optimization of injected dose and scanning protocol for 3D whole body PET/CT studies [abstract]. J Nucl Med 2004;45(suppl):426P.
32. Everaert H, Vanhove C, Lahoutte T, et al. Optimal dose of 18F-FDG required for whole-body PET using an LSO PET camera. Eur J Nucl Med Mol Imaging 2003;30:1615–1619.
33. Halpern BS, Dahlbom M, Quon A, et al. Impact of patient weight and emission scan duration on PET/CT image quality and lesion detectability. J Nucl Med 2004;45:797–801.
34. Loevinger R, Budinger TF, Watson EE. MIRD Primer for absorbed dose calculations. New York: Society of Nuclear Medicine, 1988.
35. Stabin M, Sparks R, Crowe E. OLINDA/EXM Personal Computer Code. Radiation Dose Assessment Resource (RADAR) www.dose-info-radar.com; 2004.
36. Stabin M, Siegel BA. Physical models and dose factors for use in internal dose assessment. Health Phys 2003;85:294–310.
37. Benveniste H, Fowler JS, Rooney WD, et al. Maternal-fetal in vivo imaging: a combined PET and MRI study. J Nucl Med 2003;44:1522–1530.
38. Deloar HM, Fujiwara T, Shidahara M, et al. Estimation of absorbed dose for 2-[F-18]fluoro-2-deoxy-D-glucose using whole-body positron emission tomography and magnetic resonance imaging. Eur J Nucl Med 1998;25:565–574.
39. International Commission on Radiological Protection. Radiation Dose to Patients from Radiopharmaceuticals. ICRP Publication 53. Oxford: Pergamon, 1987.
40. International Commission on Radiological Protection. Radiation Dose to Patients from Radiopharmaceuticals: Addendum 1 to ICRP53. ICRP Publication 62. Oxford: Pergamon, 1991.
41. International Commission on Radiological Protection. Radiation Dose to Patients from Radiopharmaceuticals Addendum 2 to ICRP53. ICRP Publication 80. Oxford: Pergamon, 1998.
42. International Commission on Radiological Protection. Radiation Dose to Patients from Radiopharmaceuticals Addendum 3 to ICRP53. www.icrp.org, 2000.
43. International Commission on Radiological Protection. Radiation Dose to Patients from Radiopharmaceuticals. Addenda 4-7 to ICRP Publication 53: www.icrp.org, 2001.
44. Hays MT, Watson EE, Thomas SR, et al. MIRD Dose Estimate Report No. 19: Radiation absorbed dose estimates from 18F-FDG. J Nucl Med 2002;43:210–214.
45. Hays MT, Segall GM. A mathematical model for the distribution of fluorodeoxyglucose in humans. J Nucl Med 1999;40:1358–1366.
46. Brown WD, Oakes TR, DeJesus OT, et al. Fluorine-18-fluoro-L-DOPA dosimetry with carbidopa pre-treatment. J Nucl Med 1998;39:1884–1891.

47. Brihaye C, Depresseux JC, Comar D. Radiation dosimetry for bolus administration of oxygen-15 water. J Nucl Med 1995;36:651–656.
48. Smith T, Carrison T, Lammertsma AA, et al. Dosimetry of intravenously administered oxygen-15 labelled water in man: a model based on experimental human data from 21 subjects. Eur J Nucl Med 1994;21:1126–1134.
49. Deloar HM, Watabe H, Nakamura T, et al. Internal dose estimation including the nasal cavity and major airway for continuous inhalation of C15O2, 15O2 and C15O using the thermoluminescent method. J Nucl Med 1997;38:1603–1613.
50. Thomas SR, Stabin M, Chen C-T, et al. MIRD Pamphlet No.14 revised: a dynamic urinary bladder model for radiation dose calculations. J Nucl Med 1999;40:102S–123S.
51. Dowd MT, Chen C-T, Wendel MJ, et al. Radiation dose to the bladder wall from 2-[18F] fluoro-2-deoxy-D-glucose in adult humans. J Nuc Med 1991;32:707–712.
52. Wrobel M, Carey JE, Sherman P, et al. Simplifying the dosimetry of carbon-11-labelled radiopharmaceuticals. J Nucl Med 1997;38:654–660.
53. Almeida P, Bendriem B, de Dreuille O, et al. Dosimetry of transmission measurements in nuclear medicine: a study using anthropomorphic phantoms and thermoluminescent dosimeters. Eur J Nucl Med 1998;25:1435–1441.
54. Stamm G, Nagel HD. CT-expo: a novel program for dose evaluation in CT. Rofo Fortschr Geb Rontgenstr Neuen Bildgeb Verfahr 2002;174:1570–1576.
55. ImPACT CT scanner evaluation centre. CTDosimetry.xls 0.99. Medicines and Healthcare Products Regulatory Agency (MHRA), UK, 2004.
56. Jones D, Shrimpton PC. Survey of CT Practice in the UK. Part 3: Normalised organ doses calculated using Monte Carlo techniques. NRPB-R250. Report No. NRPB-R250. National Radiological Protection Board, UK, 1991.
57. Jarry G, DeMarco JJ, Beifuss U, et al. A Monte Carlo-based method to estimate radiation dose from spiral CT: from phantom testing to patient-specific models. Phys Med Biol 2003;48:2645–2663.
58. Wu T-H, Huang Y-H, Lee JJS, et al. Radiation exposure during transmission measurement: comparison between CT- and germanium-based techniques with a current PET scanner. Eur J Nucl Med Mol Imaging 2004;31:38–43.
59. Huda W, Mergo PJ. How will the introduction of multi-slice CT affect patient doses? In: Proceedings, IAEA International Conference, Malaga 2001 Radiological Protection of Patients in Diagnostic and Interventional Radiology, Nuclear Medicine and Radiotherapy. Vienna: IAEA, 2001:202–205.
60. Hidajat N, Wolf M, Nunnemann A, et al. Survey of conventional and spiral CT doses. Radiology 2001;218:395–401.
61. Shrimpton P, Hillier MC, Lewis MH, et al. Doses from Computed Tomography (CT) Examinations in the UK: 2003 Review. NRPB-W67. Chilton, UK: National Radiological Protection Board, 2005.
62. Thomton FJ, Paulson EK, Yoshizumi TT, et al. Single versus multidetector row CT: comparison of radiation doses and dose profiles. Acad Radiol 2003;10:379–385.
63. Hamberg LM, Rhea JT, Hunter GJ, et al. Multi-detector row CT: Radiation dose characteristics. Radiology 2003;226:762–772.
64. Lewis MH. Radiation dose issues in multi-slice CT scanning. ImPACT technology update no. 3. ImPACT CT Scanner Evaluation Centre, 2004.
65. Platten D. CT issues in PET/CT scanning. ImPACT technology update no. 4. ImPACT CT Scanner Evaluation Centre, 2004.
66. Beyer T, Antoch G, Bockisch A, et al. Optimized intravenous contrast administration for diagnostic whole-body 18F-FDG PET/CT. J Nucl Med 2005;46:429–435.
67. Shrimpton PC, Jones DG, Hillier MC, et al. Survey of CT practice in the UK. Part 2: Dosimetric aspects. Report No. NRPB-R249. London: HMSO/NRPB, 1991.
68. Olerud H. Analysis of factors influencing patient dose from CT in Norway. Radiat Prot Dosim 1997;71:123–133.
69. McLean D, Malitz N, Lewis S. Survey of effective dose levels from typical paediatric CT protocols. Australas Radiol 2003;47:135–142.
70. International Commission on Radiological Protection. Radiological Protection and Safety in Medicine. ICRP Publication 73. Oxford: Pergamon, 1996.
71. MSCT. 2004 CT quality criteria: European Concerted Action on CT (FIGM-CT-2000-20078). Published at www.msct.info/CT_Quality_Criteria.htm, 2004.
72. McCollough CH, Bruesewitz MR, McNitt-Gray MF, et al. The phantom portion of the American College of Radiology (ACR) Computed Tomography (CT) accreditation program: Practical tips, artifact examples, and pitfalls to avoid. Med Phys 2004;31:2423–2442.
73. Thomas S, Stabin M, Castronovo F. Radiation-absorbed dose from 201Tl-thallous chloride. J Nucl Med 2005;46:502–508.
74. Thompson J, Tingey D. Radiation doses from computed tomography in Australia. Report No. ARL TR/123. Australian Radiation Laboratory (now Australian Radiation Protection and Nuclear Safety Agency), 1997.
75. Brix G, Lechel U, Glatting G, et al. Radiation exposure of patients undergoing whole-body dual-modality 18F-FDG PET/CT examinations. J Nucl Med 2005;46:608–613.
76. Paediatric Task Group of European Association of Nuclear Medicine. A radiopharmaceuticals schedule for imaging in paediatrics. Eur J Nucl Med 1990;17:127–129.
77. Towson JE, Smart RC, Rossleigh MA. Radiopharmaceutical activities administered for paediatric nuclear medicine procedures in Australia. Radiat Prot Australasia 2000;17:110–120.
78. Hoefnagel C, de Kraker J. Pediatric tumors. In: Ell P, Gambhir S, editors. Nuclear Medicine in Clinical Diagnosis and Treatment, 3rd ed. Edinburgh: Churchill Livingstone, 2004.
79. Cody DD, Moxley DM, Krugh KT, et al. Strategies for formulating appropriate MDCT techniques when imaging the chest, abdomen, and pelvis in pediatric patients. AJR 2004;182:849–859.
80. Hicks RJ, Binns D, Stabin MG. Pattern of uptake and excretion of 18F-FDG in the lactating breast. J Nucl Med 2001;42:1238–1242.
81. Stabin MG. Health concerns related to radiation exposure of the female nuclear medicine patient. Environ Health Perspect 1997;105(suppl 6):1403–409. Also at www.orau/ehsd/ridic.htm.
82. Stabin MG, Breitz HB. Breast milk excretion of radiopharmaceuticals: mechanisms, findings and radiation dosimetry. J Nucl Med 2000;41:863–873.
83. National Council on Radiation Protection and Measurements. Considerations regarding the unintended radiation exposure of the embryo, fetus or nursing child. NCRP Commentary No. 9. Bethesda, MD: NCRP, 1994.
84. Wagner LK, Lester RG, Saldana LR. Exposure of the Pregnant Patient to Diagnostic Radiations. A Guide to Medical Management, 2nd ed. Madison, WI: Medical Physics Publishing, 1997.
85. Russell J, Stabin M, Sparks R. Placental transfer of radiopharmaceuticals and dosimetry in pregnancy. Health Phys 1997;73:747–755.
86. Towson J, Fulham M, Eberl S, et al. Radiation dose from F18-FDG PET/CT scans in pregnancy [abstract]. Eur J Nucl Med 2004;31:S233.
87. Bohuslavizki KH, Kroger S, Klutman S, et al. Pregnancy testing before high-dose radioiodine treatment: a case report. J Nucl Med Technol 1999;27:220–221.
88. Benveniste H, Fowler JS, Rooney WD, et al. Maternal and fetal 11C-cocaine uptake and kinetics measured in vivo by combined PET and MRI in pregnant nonhuman primates. J Nucl Med 2005;46:312–320.
89. Stabin MG. Proposed addendum to previously published fetal dose estimate tables for 18F-FDG. J Nucl Med 2004;45:634–635.
90. Watson EE. Radiation absorbed dose to the human foetal thyroid. In: Proceedings, Fifth International Radiopharmaceutical Dosimetry Symposium, Oak Ridge TN, 1992. Oak Ridge: Oak Ridge Associated Universities, 1992:179–187.
91. Felmlee JP, Gray JE, Leetzow ML, et al. Estimated fetal radiation dose from multislice CT studies. AJR 1990;154:185–190.

92. Boone JM, Cooper VN, Nemzek WR, et al. Monte Carlo assessment of computed tomography dose to tissue adjacent to the scanned volume. Med Phys 2000;27:2393–2407.
93. International Commission on Radiological Protection. Radiological Protection in Biomedical Research. ICRP Publication 62. Oxford: Pergamon Press, 1991.
94. Bloe F, Williams A. Personnel monitoring observations. J Nucl Med Technol 1995;23:82–86.
95. Chiesa C, De Sanctis V, Crippa F, et al. Radiation dose to technicians per nuclear medicine procedure: comparison between technetium-99m, gallium-67 and iodine-131 radiotracers and fluorine-18 fluorodeoxyglucose. Eur J Nucl Med 1997;24:1380–1389.
96. Kearfott KJ, Carey JE, Clemenshaw MN, et al. Radiation protection design for a clinical positron emission tomography imaging suite. Health Phys 1992;63:581–589.
97. Benatar NA, Cronin BF, O'Doherty M. Radiation dose received by staff and carers/escorts following contact with 18F-FDG PET patients [abstract]. Nucl Med Commun 1999;20:462.
98. Bixler A, Springer G, Lovas R. Practical aspects of radiation safety for using fluorine-18. J Nucl Med Technol 1999;27:14–16.
99. Brown TF, Yasillo NJ. Radiation safety considerations for PET centers. J Nucl Med Technol 1997;25:98–102.
100. Dell MA. Radiation safety review for 511-keV emitters in nuclear medicine. J Nucl Med Technol 1997;25:12–17.
101. McElroy NL. Worker dose analysis based on real time dosimetry. Health Phys 1998;74:608–609.
102. Bird NJ, Barber RW, Turner KB, et al. Radiation doses to staff during gamma camera PET [abstract]. Nucl Med Commun 1999;20:471.
103. Towson J, Brackenreg J, Kenny P, et al. Analysis of external exposure to PET technologists [abstract]. Nucl Med Commun 2000;21:497.
104. Zeff B, Yester M. Patient self-attenuation and technologist dose in positron emission tomography. Med Phys 2005;32:861–865.
105. Benatar NA, Cronin BF, O'Doherty M. Radiation dose rates from patients undergoing PET: implications for technologists and waiting areas. Eur J Nucl Med 2000;27:583–589.
106. Cronin B, Marsden PK, O'Doherty MJ. Are restrictions to behaviour of patients required following fluorine-18 fluorodeoxyglucose positron emission tomographic studies? Eur J Nucl Med 1999;26:121–128.
107. Borgwardt L, Larsen HJ, Pedersen K, et al. Practical use and implementation of PET in children in a hospital PET centre. Eur J Nucl Med 2003;30:1389–1397.
108. Roberts EG, Shulkin BL. Technical issues in performing PET studies in pediatric patients. J Nucl Med Technol 2004;32:5–9.
109. McCormick VA, Miklos JA. Radiation dose to positron emission tomography technologists during quantitative versus qualitative studies. J Nucl Med 1993;34:769–772.
110. Eberl S, Anayat AA, Fulton RR, et al. Evaluation of two population-based input functions for quantitative neurological FDG PET studies. Eur J Nucl Med 1997;24:299–304.
111. Berus D, Covens P, Buls N, et al. Extremity doses of workers in nuclear medicine: mapping hand doses in function of manipulation. In: IRPA 11 International Congress Proceedings, Madrid, 2004.
112. Griff M, Berthold T, Buck A. Radiation exposure to sonographers from fluorine-18-FDG PET patients. J Nucl Med Technol 2000;28:186–187.
113. Council of the European Union. Council Directive 96/29/Euratom on basic safety standards for the protection of the health of workers and the general public. Official J Eur Commun 1996;L159:1–114.
114. International Commission on Radiation Units and Measurements. Radiation quantities and units. ICRU Report No. 33. Bethesda, MD: ICRU, 1980.
115. International Commission on Radiation Units and Measurements. Determination of Dose Equivalents Resulting from External Radiation Sources. ICRU Report No. 39. Bethesda, MD: ICRU, 1985.
116. International Commission on Radiological Protection. Conversion Coefficients for Use in Radiological Protection Against External Radiation. ICRP Publication 74. Oxford: Pergamon, 1996.
117. American National Standards Institute/American Nuclear Society. Neutron and Gamma-Ray Fluence-To-Dose Factors. Report No. ANSI/ANS-6.1.1. ANSI/ANS, 1991.
118. Shleien B, editor. The Health Physics and Radiological Health Handbook, 2nd ed. Silver Spring, MD: Scinta, 1992.
119. Cember H. Introduction to Health Physics, 3rd ed. New York: McGraw-Hill, 1996.
120. National Council on Radiation Protection and Measurements. Structural Shielding Design for Medical X-ray Imaging Facilities. Report No. 147. Bethesda, MD: NCRP, 2005.
121. National Council on Radiation Protection and Measurements. Structural Shielding Design and Evaluation for Medical Use of X-rays and Gamma Rays of Energies up to 10 MeV. Report No. 49. Bethesda, MD: NCRP, 1976.
122. Madsen M, Anderson J, Halama J, et al. AAPM Task Group on PET and PET/CT Shielding Requirements. American Association of Physicists in Medicine, 2005 release.
123. Robinson CN, Young JG, Wallace AB, et al. A study of the personal radiation dose received by nuclear medicine technologists working in a dedicated PET center. Health Phys 2005;88(suppl):S17–S21.
124. Negin C, Worku G. Microshield version 4.0: a microcomputer code for shielding analysis and dose assessment. Rockville, MD: Grove Engineering, 1992.
125. Courtney J, Mendez P, Hidalgo-Salvatierra O, et al. Photon shielding for a positron emission tomography suite. Health Phys 2001;81(suppl):S24–S28.
126. Simpkin DJ. Transmission of scatter radiation from computed tomography (CT) scanners determined by a Monte Carlo Calculation. Health Phys 1990;58:363–367.
127. Shapiro J. Radiation Protection, 3rd ed. Cambridge: Harvard University Press, 1990.
128. Zimmerman BE, Kubicek GJ, Cessna JT, et al. Radioassays and experimental evaluation of dose calibrator settings for 18F. Applied Radiat Isot 2001;54:113–122.